

## RESEARCH ARTICLE SUMMARY

## IMMUNOLOGY

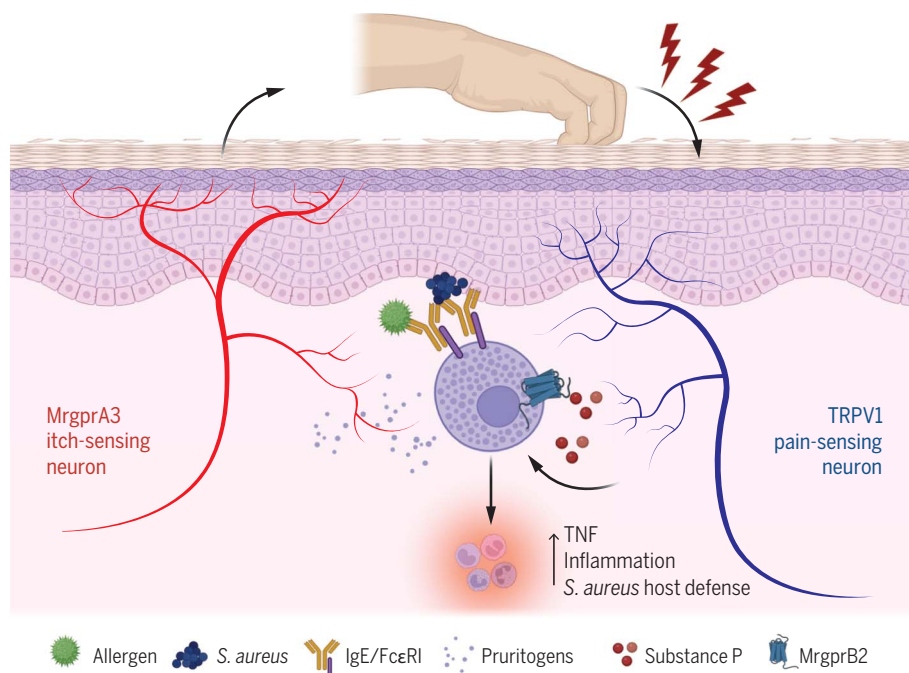
## Scratching promotes allergic inflammation and host defense via neurogenic mast cell activation

Andrew W. Liu, Youran R. Zhang, Chien-Sin Chen, Tara N. Edwards, Sumeyye Ozyaman, Torben Ramcke, Lindsay M. McKendrick, Eric S. Weiss, Jacob E. Gillis, Colin R. Laughlin, Simran K. Randhawa, Catherine M. Phelps, Kazuo Kurihara, Hannah M. Kang, Sydney-Lam N. Nguyen, Jiwon Kim, Tayler D. Sheahan, Sarah E. Ross, Marlies Meisel, Tina L. Sumpter, Daniel H. Kaplan\*

**INTRODUCTION:** Scratching is an often irresistible, stereotypical, and evolutionarily conserved behavioral response to the sensation of cutaneous itch. In many common skin diseases, such as dermatitis (eczema), protracted itching—or pruritus—is the dominant symptom and represents a substantial source of morbidity. Scratching in response to itch is clinically well recognized to exacerbate dermatitis and is pathogenic in some diseases. However, scratching an itch is often a pleasurable sensation and does not trigger avoidance behavior, which suggests that it may provide some benefit to the host.

**RATIONALE:** In the skin, activated dermal mast cells mediate hallmarks of the cutaneous allergic

response, including hives and itch, which results in scratching behavior. They also recruit inflammatory cells and promote host defense against *Staphylococcus aureus*. Mast cells can be activated through a variety of mechanisms, including allergens, that cross-link preformed complexes of immunoglobulin E (IgE) antibodies bound to the FcεRI receptor or via ligands for the MrgprB2 receptor, including substance P (SP)—a neuropeptide released by pain-sensing neurons. The functional consequence of mast cell activation through different receptors, how scratching promotes cutaneous inflammation, and whether scratching provides benefit to the host all remain poorly explored.



**Scratching synergizes with FcεRI mast cell activation to drive allergic skin inflammation.** Cross-linking of FcεRI or IgE on mast cells by allergens or *S. aureus* activates mast cell release of pruritogens (itch-inducing factors) that are sensed by MrgprA3-expressing neurons. Scratching resulting from itch sensation activates Trpv1-expressing neurons to release the neurotransmitter SP. SP acting through MrgprB2 on mast cells synergizes with FcεRI to enhance mast cell release of TNF, resulting in enhanced cutaneous inflammation and increased *S. aureus* host defense. [Figure created with BioRender.com]

**RESULTS:** To explore the relationship between itch, scratching, and inflammation, we generated mice that allow for the selective and inducible ablation of the nonpeptidergic 2 (NP2) subset of itch-sensing neurons, characterized by the expression of Mrgpra3 (called Mrgpra3<sup>DTR</sup>). We found that Mrgpra3-expressing neurons were required for scratching and inflammation in models of type 2 contact hypersensitivity and FcεRI-mediated mast cell activation. In both cases, scratching augmented mast cell degranulation, tumor necrosis factor (TNF) expression, and recruitment of neutrophils. Scratching was not required for increased expression of the alarmins thymic stromal lymphopoietin (TSLP) and interleukin-33 (IL-33), which are known to activate mast cells. Rather, we found that scratching was sufficient to trigger release of SP from Trpv1-expressing neurons that synergized with FcεRI cross-linking, resulting in maximal TNF release from mast cells. This was confirmed using mice with a genetic ablation of MrgprB2 or the gene encoding SP (*Tac1*) and by chemogenetic inhibition of Trpv1-expressing neurons. Inflammation in mice prevented from scratching could be rescued by exogenous activation of Trpv1-expressing neurons. Finally, we found that scratching reduced cutaneous microbial diversity and, in an epicutaneous *S. aureus* infection model, both inflammation and host defense required scratching.

**CONCLUSION:** The itch-scratch cycle is a pathogenic process in allergic skin rashes, such as dermatitis, or arthropod reactions. In this cycle, itch and scratching increase inflammation and disease exacerbation. Our data suggest that scratching activates cutaneous Trpv1-expressing neurons, which are a major source of SP in the skin. Coordinated activation of mast cells by both MrgprB2 and FcεRI agonism synergistically augments inflammation, in part through increased recruitment of neutrophils. Thus, dermal mast cells occupy a central node in cutaneous inflammation and are capable of integrating both adaptive and innate neuroimmune triggers. Moreover, inflammation-induced scratching can reduce the abundance of certain members of the cutaneous commensal community and, in the context of superficial *S. aureus* infection, inflammation triggered by scratching provides enhanced host defense. These data exemplify how scratching can both exacerbate disease and benefit the host through a neuroimmune axis and reconciles the seemingly paradoxical role of scratching as a pathological process and evolutionary adaptation. ■

The list of author affiliations is available in the full article online.  
\*Corresponding author. Email: dankaplan@pitt.edu  
Cite this article as A. W. Liu et al., *Science* 387, eadn9390 (2025). DOI: 10.1126/science.adn9390

**S** READ THE FULL ARTICLE AT  
<https://doi.org/10.1126/science.adn9390>

## RESEARCH ARTICLE

## IMMUNOLOGY

## Scratching promotes allergic inflammation and host defense via neurogenic mast cell activation

Andrew W. Liu<sup>1,2</sup>, Youran R. Zhang<sup>1,2</sup>, Chien-Sin Chen<sup>1,2</sup>, Tara N. Edwards<sup>1,2</sup>, Sumeyye Ozyaman<sup>1,2</sup>†, Torben Ramcke<sup>1,2</sup>, Lindsay M. McKendrick<sup>1,2</sup>, Eric S. Weiss<sup>1,2</sup>, Jacob E. Gillis<sup>1,2</sup>, Colin R. Laughlin<sup>2</sup>‡, Simran K. Randhawa<sup>2</sup>, Catherine M. Phelps<sup>2</sup>, Kazuo Kurihara<sup>1,2</sup>, Hannah M. Kang<sup>1,2</sup>, Sydney-Lam N. Nguyen<sup>1,2</sup>, Jiwon Kim<sup>3</sup>, Tayler D. Sheahan<sup>3</sup>§, Sarah E. Ross<sup>3,4</sup>, Marlies Meisel<sup>2,5</sup>, Tina L. Sumpter<sup>1,2</sup>, Daniel H. Kaplan<sup>1,2\*</sup>

Itch is a dominant symptom in dermatitis, and scratching promotes cutaneous inflammation, thereby worsening disease. However, the mechanisms through which scratching exacerbates inflammation and whether scratching provides benefit to the host are largely unknown. We found that scratching was required for skin inflammation in mouse models dependent on FcεRI-mediated mast cell activation. Scratching-induced inflammation required pain-sensing nociceptors, the neuropeptide substance P, and the mast cell receptor MrgprB2. Scratching also increased cutaneous inflammation and augmented host defense to superficial *Staphylococcus aureus* infection. Thus, through the activation of nociceptor-driven neuroinflammation, scratching both exacerbated allergic skin disease and provided protection from *S. aureus*, reconciling the seemingly paradoxical role of scratching as a pathological process and evolutionary adaptation.

Scratching is an often irresistible, stereotypical, and evolutionarily conserved behavioral response to the sensation of cutaneous itch (1). In many common skin diseases, such as dermatitis, protracted itching or pruritus—a sensation on the skin that encourages scratching—is the dominant symptom and represents a substantial source of morbidity. Scratching in response to itch is clinically well recognized to further increase pruritus and subsequent scratching, thereby exacerbating disease in a scenario called the itch-scratch cycle (2). Notably, unlike pain, which triggers avoidance and aversive behavior, scratching an itch is often pleasurable, which suggests that it may provide some benefit to the host (3). Immune cell-derived mediators, such as interleukin-4 (IL-4), IL-13, and IL-31, have been demonstrated to promote itch sensation, and blockade of their corresponding receptors is highly effective in reducing itch, scratching, and skin inflammation in patients with atopic dermatitis (4, 5). Despite these advances, the questions of

how scratching promotes cutaneous inflammation and whether scratching provides benefit to the host remain poorly explored.

Murine sensory afferent neurons innervating the skin include subsets of nociceptive, or pain-sensing, peptidergic neurons and itch-sensing nonpeptidergic neurons. Pain-sensing neurons generally express the ion channel TRPV1 and can be directly activated by numerous inflammatory cytokines and bacterial products, resulting in pain sensation (6, 7). In addition, activation of TRPV1-expressing neurons is sufficient to trigger cutaneous inflammation, and these neurons participate in many host-pathogen interactions in barrier tissues (7–9). Itch-sensing neurons include two major groupings called nonpeptidergic 2 (NP2) and nonpeptidergic 3 (NP3) (10, 11). NP3 can be identified on the basis of selective expression of the receptor for IL-31 and NP2 by expression of MrgprA3, a receptor activated by chloroquine (12–14). Receptors for other endogenous pruritogens, such as histamine from activated mast cells, IL-4 and/or IL-13 from innate lymphoid cells (ILCs) and T cells, and thymic stromal lymphopoietin (TSLP) from keratinocytes, are broadly expressed across sensory neurons (15, 16).

Mast cells are best known as effectors of anaphylactic responses. Mast cells can be activated by allergens that cross-link preformed allergen-specific immunoglobulin E (IgE) that bind to FcεRI, the high-affinity IgE receptors on their surface (17). Several endogenous factors, including the neuropeptide substance P (SP) released by pain-sensing TRPV1-expressing neurons, activate mast cells through the receptor

MrgprB2 (18). In the skin, local mast cell activation triggers the release of preformed granules containing histamine that induces local vascular permeability and edema but also triggers local pruritus (19, 20). Mast cells also trigger recruitment of inflammatory cells—most notably neutrophils—through directional release of tumor necrosis factor (TNF) into blood vessels and are required for inflammation in murine models of allergic contact dermatitis (21–23). Mast cells also mediate local host defense against *S. aureus* after either FcεRI- or MrgprB2-mediated activation (24–26). In this work, we used mouse systems to abolish the function of NP2 neurons and explore the relationship between itch, scratching, and inflammation.

### Optimal contact hypersensitivity to fluorescein isothiocyanate and oxazolone requires scratching

To generate NP2 loss-of-function mice, we bred *Mrgpra3*<sup>Cre-gfp</sup> mice with ROSA26iDTR mice to generate *Mrgpra3*<sup>DTR</sup> (13). Treatment with *Diphtheria* toxin (DT) (13, 27) ablated MrgprA3-expressing neurons (fig. S1, A and B) and reduced scratching bouts after intradermal (i.d.) administration of chloroquine, a ligand for MrgprA3, but it did not abolish scratching in response to IL-31, a ligand selective for NP3 neurons (fig. S1, C and D). Thus, DT administration efficiently and selectively ablated MrgprA3-expressing neurons in *Mrgpra3*<sup>DTR</sup> mice.

Microscopic visualization of dorsal root ganglia (DRGs) for MrgprA3 [green fluorescent protein (GFP)] and TRPV1 in *Mrgpra3*<sup>GFP</sup> mice revealed that ~60% of MrgprA3-expressing neurons did not coexpress TRPV1 (fig. S1, E and G). We also bred *Trpv1*<sup>Cre</sup> to Rosa26, hM4Di/mCitrine mice to generate *Trpv1*<sup>hM4Di</sup> inhibitory designer receptors exclusively activated by designer drugs (DREADD) mice that allow for the selective silencing of neurons after administration of clozapine *N*-oxide (CNO). RNAscope visualization of mRNA for *Mrgpra3* and mCitrine in DRGs found that ~40% of MrgprA3-expressing neurons had not undergone Cre-mediated recombination in *Trpv1*<sup>hM4Di</sup> mice (fig. S1, F and G). As expected, a single intraperitoneal (i.p.) administration of CNO suppressed nociceptor function based on delayed paw withdrawal to heat stimulation (Hargreaves test) with an effective duration of ~5.5 hours (fig. S1, H and I). However, scratching after chloroquine administration in CNO-treated *Trpv1*<sup>hM4Di</sup> mice was only partially reduced compared with *Mrgpra3*<sup>DTR</sup> mice (fig. S1C). These data were consistent with the identification of two populations of *Mrgpra3*-expressing neurons (NP2.1 and NP2.2) by transcriptomic analyses of DRGs, with NP2.1 having very low expression of *Trpv1* (28–30).

<sup>1</sup>Department of Dermatology, University of Pittsburgh, Pittsburgh, PA, USA. <sup>2</sup>Department of Immunology, University of Pittsburgh, Pittsburgh, PA, USA. <sup>3</sup>Department of Anesthesiology, University of Pittsburgh, Pittsburgh, PA, USA. <sup>4</sup>Pittsburgh Center for Pain Research, Pittsburgh, PA, USA. <sup>5</sup>Cancer Immunology and Immunotherapy Program, UPMC Hillman Cancer Center, Pittsburgh, PA, USA.

\*Corresponding author. Email: dankaplan@pitt.edu

†Present address: Department of Histology and Embryology, School of Medicine, Istanbul Medipol University, Istanbul, Turkey.  
‡Present address: Department of Immunobiology, Yale University, New Haven, CT, USA.

§Present address: Department of Cell Biology, Neurobiology and Anatomy, Medical College of Wisconsin, Milwaukee, WI, USA.

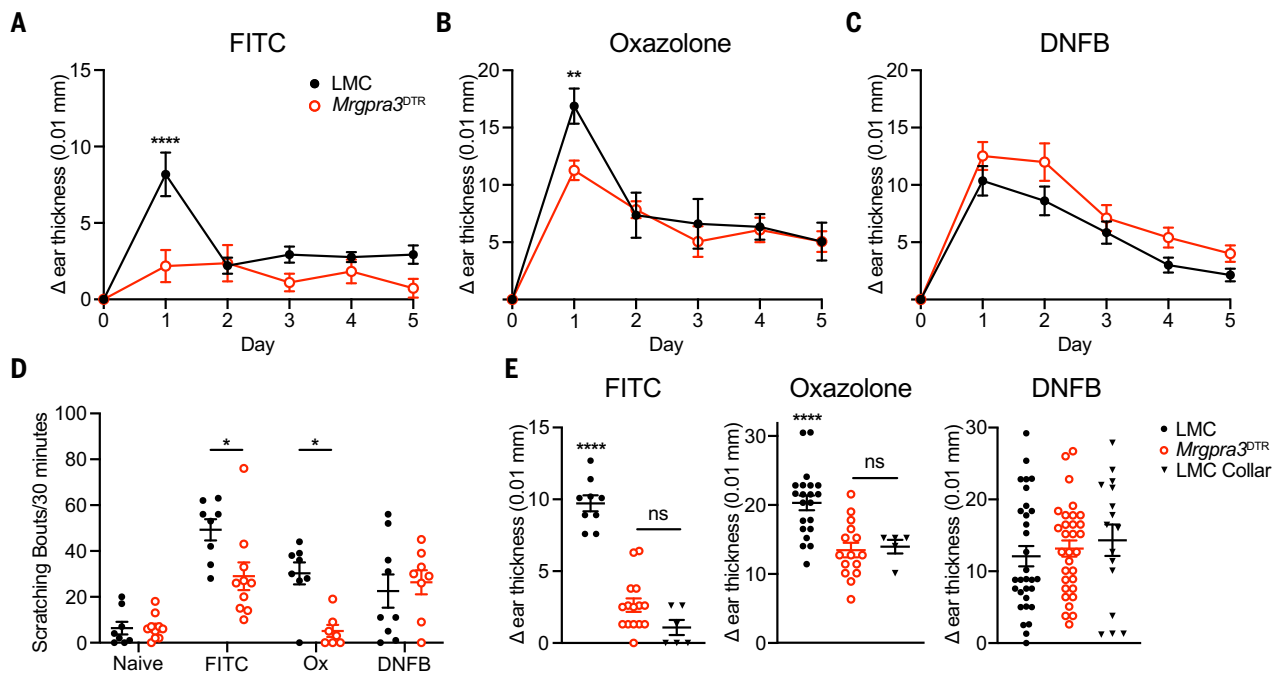


**Fig. 1. *MrgprA3*-expressing neurons and scratching are required for FITC and Ox CHS.** (A to C) DT-treated *Mrgpra3<sup>DTR</sup>* (red circles) or LMC (black circles) mice were sensitized on shaved abdominal skin with FITC (LMC and *Mrgpra3<sup>DTR</sup>*  $n = 7$  mice) (A), Ox (LMC and *Mrgpra3<sup>DTR</sup>*  $n = 10$ ) (B), or DNFB (LMC and *Mrgpra3<sup>DTR</sup>*  $n = 27$ ) (C) hapten followed by challenge 5 days later on the ear with the same hapten. Ear thickness at the indicated time points after challenge is shown (FITC LMC and *Mrgpra3<sup>DTR</sup>*  $n = 7$ ; Ox LMC and *Mrgpra3<sup>DTR</sup>*  $n = 10$ ; DNFB LMC  $n = 9$  and DNFB *Mrgpra3<sup>DTR</sup>*  $n = 8$ ). (D) The number of scratching bouts observed over 30 min in mice 1 day postchallenge, with the indicated hapten shown (LMC  $n = 8$  to 9, *Mrgpra3<sup>DTR</sup>*  $n = 7$  to 10). (E) Ear thickness 1 day after

hapten challenge in DT-treated LMC and *Mrgpra3<sup>DTR</sup>* mice as well as Elizabethan-collared control mice (LMC collar; black triangles) is shown (FITC, LMC  $n = 9$ , *Mrgpra3<sup>DTR</sup>*  $n = 15$ , collar  $n = 6$ ; Ox, LMC  $n = 20$ , *Mrgpra3<sup>DTR</sup>*  $n = 15$ , collar  $n = 5$ ; DNFB, LMC and *Mrgpra3<sup>DTR</sup>*  $n = 31$ , collar  $n = 17$ ). Results in (A) to (C) are represented as means  $\pm$  SEMs from three to five independent experiments. Individual data points in (D) and (E) represent data from a single animal, and bars are means  $\pm$  SEMs from three to five independent experiments. Significance was calculated using unpaired Student's *t* test [(A) to (C)], Mann-Whitney (D), or one-way analysis of variance (ANOVA) with multiple comparisons (E). \* $P < 0.05$ ; \*\* $P < 0.01$ ; \*\*\*\* $P < 0.0001$ ; ns, not significant.

To determine whether *MrgprA3*-expressing neurons were required for contact hypersensitivity (CHS), a model for allergic contact dermatitis *Mrgpra3<sup>DTR</sup>* and littermate control (LMC) mice were treated with DT, sensitized on the shaved abdomen with the haptens fluorescein isothiocyanate (FITC), oxazolone (Ox), or dinitrofluorobenzene (DNFB). Five days later, mice were challenged on the ear with the same hapten, and ear thickness was measured as a surrogate for inflammation. Ear thickness in response to all three haptens peaked 1 day postchallenge and was reduced in *Mrgpra3<sup>DTR</sup>* mice treated with FITC and Ox but not DNFB (Fig. 1, A to C). To determine whether *MrgprA3*-expressing neurons were required during the challenge phase, we adjusted our protocol to administer DT 3 and 6 days after sensitization and challenged mice on day 8. Effective ablation of *MrgprA3*-expressing neurons was confirmed by reduced chloroquine-induced scratching (fig. S1J). CHS to FITC and Ox were both reduced, indicating that *MrgprA3*-expressing neurons were required during the challenge phase of CHS (fig. S1, K and L).

We hypothesized that reduced inflammation in *Mrgpra3<sup>DTR</sup>* could be related to the loss of

scratching. Scratching behavior was reduced in DT-treated *Mrgpra3<sup>DTR</sup>* in response to FITC and Ox but not DNFB (Fig. 1D). This was confirmed by repeating these experiments with LMC control mice wearing Elizabethan collars to physically prevent scratching at the time of challenge. Mice with reduced responses to itch-inducing agents (*Mrgpra3<sup>DTR</sup>* mice) or mice that could not scratch (LMC collar) failed to develop robust ear inflammation in response to FITC and Ox but not DNFB (Fig. 1E). On the basis of these data, we concluded that in response to a subset of haptens, scratching and the development of robust CHS inflammation required *MrgprA3*-expressing neurons.

#### Scratching is required for optimal neutrophil infiltration and mast cell degranulation

To understand how scratching augmented inflammation, we examined ears 1 day after hapten challenge by histological analysis. Both FITC- and Ox-challenged ears in LMC mice showed edema and a mostly neutrophilic infiltrate, with FITC-treated mice having more edema and Ox-treated mice having a greater infiltrate (Fig. 2A). The cellular infiltrate and number of neutrophils were substantially decreased

based on histology and flow cytometry in both *Mrgpra3<sup>DTR</sup>* mice and LMC mice wearing collars (Fig. 2, B and C, and fig. S2, A to C). In CHS, TNF is required for the recruitment of neutrophils into the skin (31, 32). Expression of *Tnf* was increased after FITC and Ox challenge in LMC mice but not in *Mrgpra3<sup>DTR</sup>* mice or LMC mice wearing collars (Fig. 2, D and E). Expression of *Tslp*, which can be increased by barrier disruption (15, 33, 34), was elevated by hapten challenge in all groups but was not dependent on *MrgprA3*-expressing neurons or scratching (fig. S2, D and E). Alterations in cellular infiltrate and *Tnf* expression were not observed with DNFB CHS (fig. S2, H to J). FITC CHS responses were unaffected by inhibition of calcitonin gene-related peptide (CGRP) (fig. S2G).

Because the peak of CHS inflammation was at 24 hours postchallenge, key mechanistic events might be occurring at earlier time points. Thus, ear thickness after FITC and Ox challenge was measured starting at 1 hour postchallenge (Fig. 2, F and G). Differences in inflammation were even more pronounced, with reduced ear thickness in *Mrgpra3<sup>DTR</sup>* mice and collared LMC mice first evident at 10 to 12 hours after

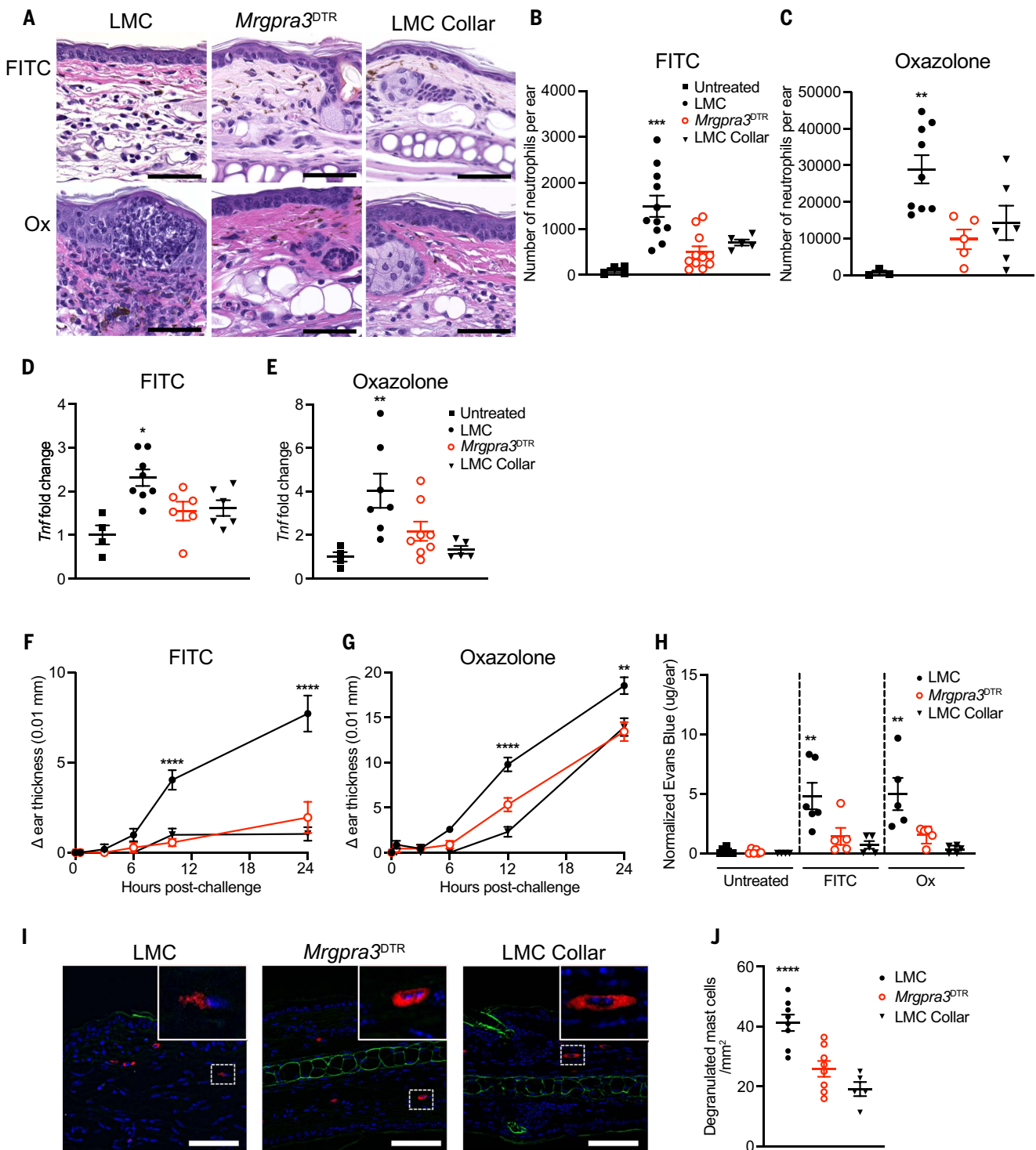


**Fig. 2. Scratching is required for neutrophilic infiltrate and mast cell activation.** (A) Representative H&E sections of ears from sensitized DT-treated LMC (black circles), *Mrgpra3<sup>DTR</sup>* (red circles), and collared LMC (black triangles) mice 24 hours after FITC or Ox challenge. (B) The total number of neutrophils from untreated mice, FITC-challenged DT-treated LMC, *Mrgpra3<sup>DTR</sup>*, and collared LMC mice at 24 hours, as determined by flow cytometry (untreated  $n = 4$ , LMC and *Mrgpra3<sup>DTR</sup>*  $n = 11$ , collar  $n = 5$ ). (C) Same as in (B) but sensitized and challenged with Ox (untreated  $n = 3$ , LMC  $n = 9$ , *Mrgpra3<sup>DTR</sup>*  $n = 5$ , collar  $n = 6$ ). (D and E) Relative expression of *Tnf* mRNA based on quantitative reverse transcription PCR (RTqPCR) of whole ear skin from unmanipulated, *Mrgpra3<sup>DTR</sup>*,

and collared LMC mice 24 hours after FITC (untreated  $n = 4$ , LMC  $n = 8$ , *Mrgpra3<sup>DTR</sup>* and collar  $n = 6$ ) (D) and Ox challenge (untreated  $n = 4$ , LMC and *Mrgpra3<sup>DTR</sup>*  $n = 8$ , collar  $n = 5$ ) (E). (F and G) Ear thickness at the indicated time points after FITC (LMC  $n = 17$ , *Mrgpra3<sup>DTR</sup>*  $n = 18$ , collar  $n = 11$ ) (F) and Ox (LMC  $n = 36$ , *Mrgpra3<sup>DTR</sup>*  $n = 20$ , collar  $n = 10$ ) (G) challenge is shown. (H) Quantification of EB dye extravasation in FITC- or Ox-sensitized DT-treated LMC, *Mrgpra3<sup>DTR</sup>*, and collared LMC mice 10 hours after FITC challenge and 12 hours after Ox challenge (LMC  $n = 7$ , *Mrgpra3<sup>DTR</sup>* and collar  $n = 5$ ). (I) Immunofluorescent microscopic visualization of ear skin 10 hours after FITC challenge illustrates avidin<sup>+</sup> mast cells (red) and DAPI nuclear label (blue) in

DT-treated LMC, *Mrgpra3*<sup>DTR</sup>, and LMC collared mice. Background FITC appears green. Regions highlighted by dotted lines are shown at higher magnification in insets. (J) Quantification of the number of degranulated mast cells observed in (I) is shown (LMC and *Mrgpra3*<sup>DTR</sup> *n* = 8, collar *n* = 5). Scale bars [(A) and (I)], 200  $\mu$ m. Individual data points represent data from a single animal, and bars

show means  $\pm$  SEMs from three independent experiments [(B) to (E), (H), and (J)]. Results in (F) and (G) are represented as means  $\pm$  SEMs from three independent experiments. Significance was calculated using a one-way ANOVA with multiple comparisons [(B) to (H) and (J)]. \**P* < 0.05; \*\**P* < 0.01; \*\*\**P* < 0.001; \*\*\*\**P* < 0.0001.

FITC and Ox but not after DNFB challenge (fig. S2K).

The rapid time course, coupled with histologic evidence of edema and the known role for mast cell–derived TNF in neutrophil recruitment, suggested that scratching-induced mast cell degranulation could explain our observations (21, 32, 35). As expected, FITC CHS was reduced in mast cell–deficient mice (fig. S2L) (23, 36, 37). Both FITC and Ox challenge triggered local extravasation of Evans blue (EB) dye, a measurement of dermal edema at 12 hours postchallenge in LMC mice (Fig. 2H). EB extravasation was reduced almost to baseline in *Mrgpra3*<sup>DTR</sup> mice and LMC mice wearing collars despite numbers of dermal mast cells remaining unchanged (fig. S2F). Visualization of mast cell granules with avidin—which binds to abundant negatively charged proteoglycans found in mast cell granules, thereby allowing for easy identification of these cells—confirmed a decrease in the percentage of degranulated mast cells in the absence of scratching (Fig. 2, I and J). On the basis of these data, we concluded that in both FITC and Ox CHS, scratching was required for inflammation, mast cell degranulation, expression of *Tnf*, and recruitment of neutrophils into the skin.

### Passive cutaneous anaphylaxis inflammation is amplified by scratching

To directly assess how scratching was required for mast cell activation in vivo, we activated mast cells with MrgprB2 agonism through injection of SP or compound 48/80, a synthetic ligand for MrgprB2, into the dermis of wild-type (WT) mice. Moderate transient scratching that required MrgprA3-expressing neurons was evident at 30 min (Fig. 3A and fig. S3A). Increased ear thickness resulting from edema was also evident at 30 min and resolved by 10 hours with no requirement for scratching (Fig. 3B and fig. S3B). To activate mast cells through Fc $\epsilon$ RI, we performed a passive cutaneous anaphylaxis (PCA) assay in which we first sensitized the ear pinna with dinitrophenyl-specific IgE and followed up with a treatment of dinitrophenyl-albumin (DNP) 20 hours later (38). During the early response after DNP, scratching but not edema-mediated ear swelling was reduced in *Mrgpra3*<sup>DTR</sup> mice. Notably, at the 10-hour time point, which is characterized by neutrophilic infiltration (31), we observed reduced ear thickness and less edema in *Mrgpra3*<sup>DTR</sup> and collared LMC mice (Fig. 3, C to E). A reduced neutrophilic infiltrate at the 10-hour time point was confirmed

by visualization of neutrophils with anti-Gr1 (Fig. 3, F and G). Consistent with reduced numbers of neutrophils, expression of *Tnf* mRNA and TNF protein were reduced in *Mrgpra3*<sup>DTR</sup> mice and LMC mice wearing collars compared with uncollared LMC mice (Fig. 3, H and I).

These data align well with the requirement for scratching in the FITC and Ox but not DNFB CHS models. Unlike DNFB, both FITC and Ox have been reported to trigger type 2 responses, as evidenced by increased IgE production (fig. S3C) (39–41). This raised the possibility that scratching could synergize with Fc $\epsilon$ RI-mediated mast cell activation to increase TNF, neutrophil recruitment, and inflammation.

### TRPV1-expressing nociceptors and SP are required for scratching-induced mast cell activation

To understand how scratching promoted Fc $\epsilon$ RI-mediated mast cell activation, we examined levels of TSLP and IL-33. Both cytokines can be released by keratinocytes in response to epidermal disruption and have been reported to stimulate mast cell activation (33, 34, 42–45). Protein expression of TSLP and IL-33 measured in ear tissue 10 hours after Fc $\epsilon$ RI-mediated mast cell activation were equally elevated in both LMC and collared LMC mice compared with untreated controls, which indicates that expression was unrelated to scratching (fig. S4, A and B). By contrast, Fc $\epsilon$ RI-mediated mast cell activation in the PCA assay triggered release of SP to levels similar to those obtained with activation of Trpv1-expressing neurons by administration of capsaicin and was attenuated in collared mice that were prevented from scratching (Fig. 4A).

On the basis of this finding, we hypothesized that MrgprB2 ligation by SP could augment Fc $\epsilon$ RI-mediated mast cell activation. To test this, we turned to primary peritoneal mast cell cultures (PMCs), a common in vitro surrogate for connective tissue mast cells (46). PMCs efficiently degranulate and release  $\beta$ -hexosaminidase ( $\beta$ -hex), which is found in granules in response to both Fc $\epsilon$ RI cross-linking and MrgprB2 agonism (47, 48). By contrast, Fc $\epsilon$ RI cross-linking is much more effective than MrgprB2 agonism for the release of TNF (38).

To determine whether there was a combinatorial effect, we treated PMCs with anti-dinitrophenyl IgE followed by increasing concentrations of DNP and/or compound 48/80. Analysis of supernatants 6 hours poststimulation

confirmed that DNP or compound 48/80 in isolation led to similar degranulation based on  $\beta$ -hex release, but only DNP induced appreciable TNF release (Fig. 4, B and C, and fig. S4, C and D). At the DNP dose of 100 ng/ml, the addition of compound 48/80 only led to a slightly increased  $\beta$ -hex release, but notably, the addition of compound 48/80 led to a synergistic release of TNF (Fig. 4, B and C). Similar results were obtained combining DNP with SP (fig. S4E).

Because peritoneal cell–derived mast cells are not fully equivalent to dermal mast cells, we next determined whether MrgprB2 ligation affected mast cell function after Fc $\epsilon$ RI cross-linking in vivo by repeating the PCA assay in mice lacking MrgprB2 (*Mrgprb2*<sup>−/−</sup>) and mice lacking the gene encoding SP and neurokinin A (*Tac1*<sup>−/−</sup>). Ear thickness at 10 hours, edema based on EB extravasation, and expression of *Tnf* were all reduced (Fig. 4, D to F). Similar results were obtained in WT mice by administration of QWF, an inhibitor of SP receptors. Notably, scratching was unaffected in *Mrgprb2*<sup>−/−</sup>, *Tac1*<sup>−/−</sup>, or QWF-treated WT mice (Fig. 4G). Thus, SP, *Tac1*, and other MrgprB2 ligands were dispensable for mast cell–induced scratching after Fc $\epsilon$ RI-mediated mast cell activation. Moreover, the decoupling of scratching from inflammation established that SP and its receptor on mast cells, MrgprB2, were required for inflammation downstream of scratching behavior.

TRPV1-expressing nociceptors are a major source of SP in the skin, which can be released by scratching (12, 49–51). To determine whether nociceptors were required for scratching-induced inflammation, we repeated the PCA assay in *Trpv1*<sup>hM4Di</sup> inhibitory DREADD mice. PCA responses at 10 hours in CNO-treated *Trpv1*<sup>hM4Di</sup> mice showed reduced release of SP, reduced ear thickness, reduced edema, and reduced expression of *Tnf* compared with CNO-treated control mice (Fig. 4, A and H to J). As with inhibition of SP receptors and ablation of *Mrgprb2* or *Tac1*, scratching behavior was unaffected (Fig. 4K). We confirmed that scratching in response to FITC CHS was unaffected in CNO-treated *Trpv1*<sup>hM4Di</sup> mice (fig. S4F). These data supported a model in which scratching triggers nociceptor activation resulting in SP release, though a nonneuronal source of SP has not been formally excluded. SP engagement of MrgprB2 on mast cells then synergizes with Fc $\epsilon$ RI cross-linking to augment the release of TNF, thereby triggering increased neutrophil recruitment and increased inflammation (fig. S5).

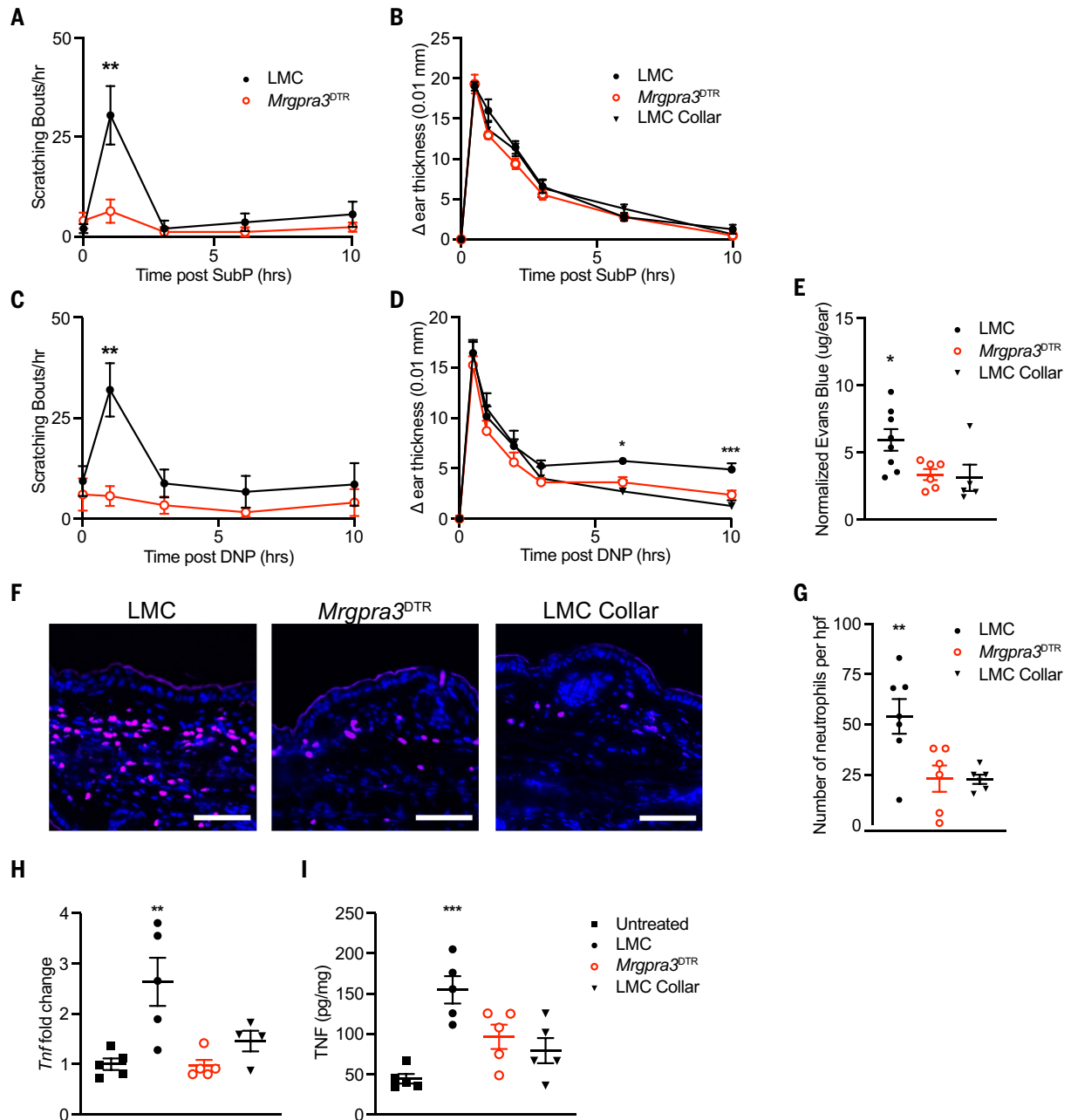


**Fig. 3. Scratching is required for neutrophilic inflammation after Fc $\epsilon$ RI-mediated mast cell activation.** (A) The number of scratching bouts per hour in DT-treated LMC (black circles) and *Mrgpra3<sup>DTR</sup>* (red circles) at the indicated time after i.d. injection of 1.2  $\mu$ g of SP ("SubP") into the ear is shown. (B) Ear thickness in DT-treated LMC, *Mrgpra3<sup>DTR</sup>*, and collared LMC (black triangles) mice at the indicated time after i.d. injection of SP into the ear is shown (LMC  $n = 9$ , *Mrgpra3<sup>DTR</sup>*  $n = 5$ , collar  $n = 4$ ). (C and D) Same as in (A) and (B) except mice were sensitized with 20 ng of dinitrophenyl-specific IgE followed by i.d. injection of 2  $\mu$ g of DNP to the ear pinna 20 hours later (LMC  $n = 10$  to 15, *Mrgpra3<sup>DTR</sup>*  $n = 7$  to 11, collar  $n = 6$ ). (E) Quantification of EB dye extravasation 10 hours after DNP challenge (LMC  $n = 8$ , *Mrgpra3<sup>DTR</sup>*  $n = 6$ , collar  $n = 5$ ). (F) Immunofluorescent microscopic visualization with DAPI (blue) and anti-Gr1

(magenta) to visualize neutrophils in ear skin 10 hours after DNP challenge. (G) Quantification of numbers of neutrophils in (F) is shown (LMC  $n = 7$ , *Mrgpra3<sup>DTR</sup>*  $n = 6$ , collar  $n = 5$ ). (H and I) Expression of normalized *Tnf* mRNA (H) and TNF protein expression (I) in whole ear skin from unmanipulated mice (black squares) and DT-treated LMC, *Mrgpra3<sup>DTR</sup>*, and LMC collared mice 10 hours after DNP challenge (untreated  $n = 4$ ; LMC, *Mrgpra3<sup>DTR</sup>*, and collar  $n = 5$ ). Scale bar (F), 200  $\mu$ m. Results in (A) to (D) are represented as means  $\pm$  SEMs from three independent experiments. Individual data points [(E) and (G) to (I)] represent data from a single animal, and bars show means  $\pm$  SEMs from three independent experiments. Significance was calculated using a Mann-Whitney test [(A) and (C)] or by one-way ANOVA with multiple comparisons [(B), (D), (E), and (G) to (I)]. \* $P < 0.05$ ; \*\* $P < 0.01$ ; \*\*\* $P < 0.001$ ; \*\*\*\* $P < 0.0001$ .

A prediction of this model is that nociceptor activation should compensate for the absence of scratching. To test this, we performed the PCA assay on collared and uncollared WT

mice but mixed the DNP challenge with either vehicle or capsaicin to activate TRPV1-expressing neurons. As before, collared mice failed to develop increased ear thickness, EB

extravasation, or increased expression of *Tnf*. The addition of capsaicin, however, rescued all of these parameters back to the level of the uncollared cohort, and this rescue was

#### Fig. 4. Scratching-induced inflammation requires neurogenic mast cell activation.

(A) WT (black circles), collared WT (black triangles), and *TrpV1<sup>hM4Di</sup>*

(blue triangles) mice were challenged with DNP and quantification of SP in supernatants from ex vivo skin explant organ cultures of ear tissue harvested 30 min after challenge. Unchallenged (black squares) and collared mice treated with capsaicin (open squares) are also shown (unchallenged, capsaicin, and DNP collar  $n = 8$ ; DNP  $n = 16$ ; *TrpV1<sup>hM4Di</sup>*  $n = 6$ ).

(B and C) Percentage of mast cell degranulation as calculated by  $\beta$ -hex release (B) and TNF protein levels (in picograms per milliliter) (C) from the culture supernatants of DNP-specific IgE-sensitized cultured PMCs from six mice across three experiments 6 hours after treatment with the indicated dose of DNP and 48/80. (D to F) Ear thickness (D), quantification of EB extravasation (E), and *Tnf* mRNA (F) measured at 10 hours after DNP challenge in vehicle-treated (black circles), QWF-treated (magenta circles), *MrgprB2<sup>-/-</sup>* (purple circles), and *Tac1<sup>-/-</sup>* (lavender circles) DNP-specific IgE-sensitized mice. (G) Scratching behavior over 30 min after DNP challenge in vehicle-treated, QWF-treated, *MrgprB2<sup>-/-</sup>*, and *Tac1<sup>-/-</sup>* mice (vehicle  $n = 9$  to 13, QWF  $n = 7$ , *MrgprB2<sup>-/-</sup>*  $n = 8$  to 12, *Tac1<sup>-/-</sup>*  $n = 9$ ).

(H to J) Ear thickness (H), quantification of EB extravasation (I), and *Tnf* mRNA (J) measured at 10 hours after DNP challenge in CNO-treated LMC and *TrpV1<sup>hM4Di</sup>* mice (LMC  $n = 7$  to 10, *TrpV1<sup>hM4Di</sup>*  $n = 8$  to 9).

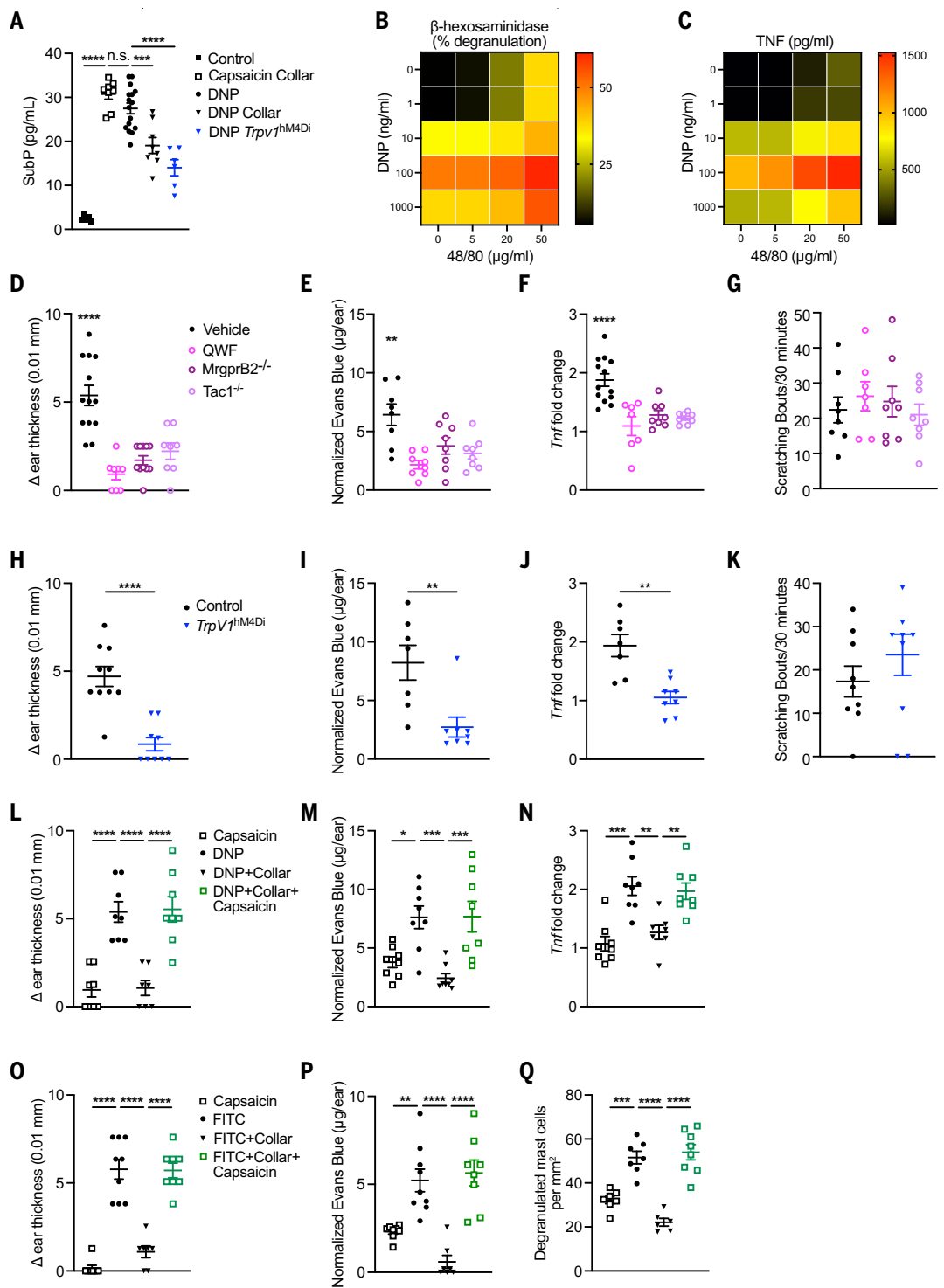
(K) Scratching behavior over 30 min after DNP challenge. (L to N) Ear thickness (L), quantification of EB extravasation (M), and *Tnf* mRNA (N) measured at 10 hours after capsaicin treatment (black squares), DNP challenge (black circles), DNP challenge in collared mice (black triangles), and DNP and capsaicin in collared mice (green squares) (capsaicin, DNP, and DNP capsaicin collar  $n = 8$ ; DNP collar  $n = 7$ ).

(O to Q) Ear thickness (O), quantification of EB extravasation (P), and degranulated mast cells (Q) quantified at 10 hours after FITC challenge in cohorts, as in (L) to (N) (capsaicin  $n = 7$  to 8, FITC  $n = 7$  to 9, collar  $n = 6$  to 7, FITC capsaicin collar  $n = 8$ ). Individual data points represent data from a single animal, and bars show means  $\pm$  SEMs from three independent experiments. Significance was calculated using a one-way ANOVA with multiple comparisons [(A), (D) to (G), and (L) to (Q)], unpaired Student's *t* test [(H) to (J)], or Mann-Whitney test (K). \* $P < 0.05$ ; \*\* $P < 0.01$ ; \*\*\* $P < 0.001$ ; \*\*\*\* $P < 0.0001$ .

inhibited in *Mrgprb2<sup>-/-</sup>* mice (Fig. 4, L to N, and fig. S4, I to K). Similarly, the addition of capsaicin to FITC during the CHS challenge phase rescued inflammation, EB extravasa-

tion, and mast cell degranulation in collared mice with the numbers of dermal mast cells remaining unchanged (Fig. 4, O to Q, and fig. S4, G and H). Thus, nociceptor activation

can rescue inflammation in the absence of scratching, thereby demonstrating a neurogenic mechanism linking scratching with allergic inflammation.



### MrgprA3-expressing neurons and scratching are required for optimal host defense to *S. aureus*

Colonization and superficial infection with *S. aureus* along with alterations of the cutaneous microbiome are strongly associated with the development of atopic dermatitis (52–57). Given the link between scratching and allergic inflammation, we hypothesized that scratching could affect the cutaneous microbiome. To test this, cohorts of DT-treated *Mrgpra3*<sup>DTR</sup>, LMC, and collared LMC mice were sensitized and challenged with FITC using our CHS model. At 24 hours postchallenge, both the challenged and nonchallenged (i.e., unmanipulated) ears were harvested under sterile conditions. We assessed the skin microbiome composition using two parallel approaches: To globally profile the presence of bacterial signatures, we performed 16S ribosomal RNA sequencing (16S rRNA-seq) of skin microbial DNA, and to broadly delineate the viable skin microbiome, we used a culturomics approach using broths and agars of diverse nutrient composition, enabling recovery of low-abundance and phylogenetically distinct bacteria (58).

Based on analysis of 16S rRNA-seq of unmanipulated ears, we found that the presence of collars for 24 hours on LMC mice had minimal impact on microbial diversity. However, the microbial diversity of *Mrgpra3*<sup>DTR</sup> mice differed from LMC mice as shown in a species-level diversity graph and the average Bray Curtis  $\beta$ -diversity (fig. S6, A and B, and fig. S7). We found a reduction in alpha diversity, a measurement of the number of microbial taxa (richness) between FITC challenged and contralateral unmanipulated ears, which was absent in collared LMC and *Mrgpra3*<sup>DTR</sup> mice where scratching was not present (Fig. 5A). LEfSe analysis (linear discriminant analysis effect size) revealed a decrease in specific taxa within the phylum *Firmicutes*, which suggests that scratching could reduce *Firmicutes* abundance (Fig. 5B and fig. S8). Culturomic analysis (fig. S9) revealed the presence of nine viable genera, including *Staphylococcus* from unmanipulated LMC ears (Fig. 5C). Notably, in FITC-treated ears from LMC mice, we observed a loss of *Staphylococcus*, *Lysinibacillus*, and *Ligilactobacillus*, which was not evident in FITC-treated collared mice. Thus, using two independent but complementary techniques, we have demonstrated that scratching induced by FITC CHS reduced the abundance of specific members of the cutaneous commensal community, including viable *Staphylococcus*.

Recently, the V8 protease has been identified as a major *S. aureus*-derived factor that drives pruritus through engagement with the PAR1 receptor (30). MrgprA3-expressing neurons innervate the epidermis, and a subset also expresses *F2r*, the gene for PAR1 (12, 13, 30). To test whether V8 protease-mediated scratching

required MrgprA3-expressing neurons, 40 U of recombinant V8 protease was intradermally injected into the nape of DT-treated *Mrgpra3*<sup>DTR</sup> and LMC mice. V8 protease induced a robust scratching response, which was reduced in the absence of MrgprA3-expressing neurons (Fig. 5D). Next, using a modified *S. aureus* infection model (30, 59), we skin-infected DT-treated *Mrgpra3*<sup>DTR</sup> and LMC mice with 10<sup>7</sup> colony-forming units (CFU) of *S. aureus* USA300 under an occlusive patch that allows for epidermal infection. Five days later, spontaneous scratching immediately after patch removal and allodnesis at 10 hours were measured (fig. S6C and Fig. 5, E and F). Both were reduced in the absence of MrgprA3-expressing neurons.

We repeated the experiment but waited a further 9 days after patch removal to allow an adaptive immune response to develop, which was confirmed by increased serum IgE (fig. S6D). Mice were then challenged by pricking the ventral ears eight times using allergen needles coated with 10<sup>9</sup> CFU *S. aureus* (25). Within 30 min, naïve LMC mice exhibited modest MrgprA3-dependent site-directed scratching behavior, which was increased in sensitized mice (Fig. 5G). At 8 hours after *S. aureus* challenge, sensitized LMC control mice showed increased ear thickness, edema, *Trf* expression, and mast cell degranulation (Fig. 5, H to K). Notably, these parameters were all reduced in collared LMC and *Mrgpra3*<sup>DTR</sup> mice. Because IgE-mediated mast cell activation provides host defense against *S. aureus* (25), we assessed total bacterial load in the ear 1 day after *S. aureus* challenge. In naïve, unpatched mice, scratching did not affect CFU (Fig. 5L). By contrast, CFU was reduced by ~10-fold in sensitized mice. Notably, this protection was lost in *Mrgpra3*<sup>DTR</sup> and collared mice. Thus, in sensitized mice with elevated IgE, optimal mast cell activation, cutaneous inflammation, and *S. aureus* host defense all required itch sensation and scratching.

### Discussion

The itch-scratch cycle is a pathogenic process in pruritic allergic skin rashes or lesions, such as from dermatitis or an arthropod bite. In this cycle, itching and scratching increase inflammation and disease exacerbation. We now provide a mechanistic underpinning for this effect. Scratching activates cutaneous TRPV1-expressing neurons, which are a major source of SP in the skin. Coordinate activation of mast cells by both MrgprB2 and Fc $\epsilon$ RI agonism synergistically augments inflammation, at least in part through increased recruitment of neutrophils. Thus, dermal mast cells occupy a central node in cutaneous inflammation and are capable of integrating both adaptive and innate neuroimmune triggers. Moreover, inflammation-induced scratching can reduce the abundance of certain members of the cutaneous commensal community and, in the context of superficial

*S. aureus* infection, augmented inflammation triggered by scratching provides enhanced host defense. Thus, these data exemplify how scratching can exacerbate dermatitis and benefit the host through a neuroimmune axis.

The pathogenic role of scratching in diseases such as atopic dermatitis appears to be at odds with the evolutionary conservation of scratching and the pleasurable sensation of scratching an itch, thereby suggesting that there is a host benefit from scratching (3). The finding that scratching reduced *S. aureus* burden in the context of infection demonstrates a benefit from scratching that was previously lacking. Scratching also affected the cutaneous microbiome, which may prove important in preventing dysbiosis. Notably, mice lacking MrgprA3-expressing neurons appeared to have dysbiosis. In our acute scratching models, we did not observe an outgrowth of *S. aureus*, which is commonly seen in atopic dermatitis. Atopic dermatitis, however, is a chronic disease involving dysregulation of the epidermal barrier, immune system, and the cutaneous microbiome. The role of mast cells in the pathogenesis of atopic dermatitis remains controversial. Thus, although we have demonstrated that scratching suppressed *S. aureus* burden in the acute context, there are many other factors that likely allow for its overgrowth in the context of chronic disease.

Scratching was largely abrogated in MrgprA3 or NP2 loss-of-function mice in response to direct mast cell activation through MrgprB2 or Fc $\epsilon$ RI ligation, which is consistent with prior observations (47). In more complex models, loss of NP2 neurons had more variable results, with partial inhibition of scratching in FITC CHS, V8 protease, and superficial *S. aureus* infection whereas DNFB CHS was unaffected. This likely results from pruritogens not derived from mast cells activating the NP3 neuron subset, which remains intact in *Mrgpra3*<sup>DTR</sup> mice. *Trpv1* is transiently expressed during ontogeny, resulting in broad expression of Cre in most sensory afferents, including some NP2 neurons (60). Thus, it was unexpected that scratching in response to PCA or FITC CHS was not affected in CNO-treated *Trpv1*<sup>hM4Di</sup>. Single-cell analysis of DRG transcripts indicates that a subset of *Mrgpra3*-expressing neurons (NP2.1) expresses very low levels of *Trpv1* compared with the NP2.2 subset, although *Trpv1* expression was not observed in analysis of bulk-sorted MrgprA3-expressing neurons (28, 60). NP2.1 neurons also express transcripts for *F2r* (PAR1), which senses *S. aureus* V8 protease and *Mrgprb4*, which is associated with pleasurable touch sensation (61). This aligns with our observation that ~60% of MrgprA3-expressing neurons do not coexpress TRPV1. In addition, in *Trpv1*<sup>hM4Di</sup> mice, ~40% of MrgprA3-expressing neurons do not coexpress *Trpv1*, and scratching in response to chloroquine was only partially reduced. We speculate

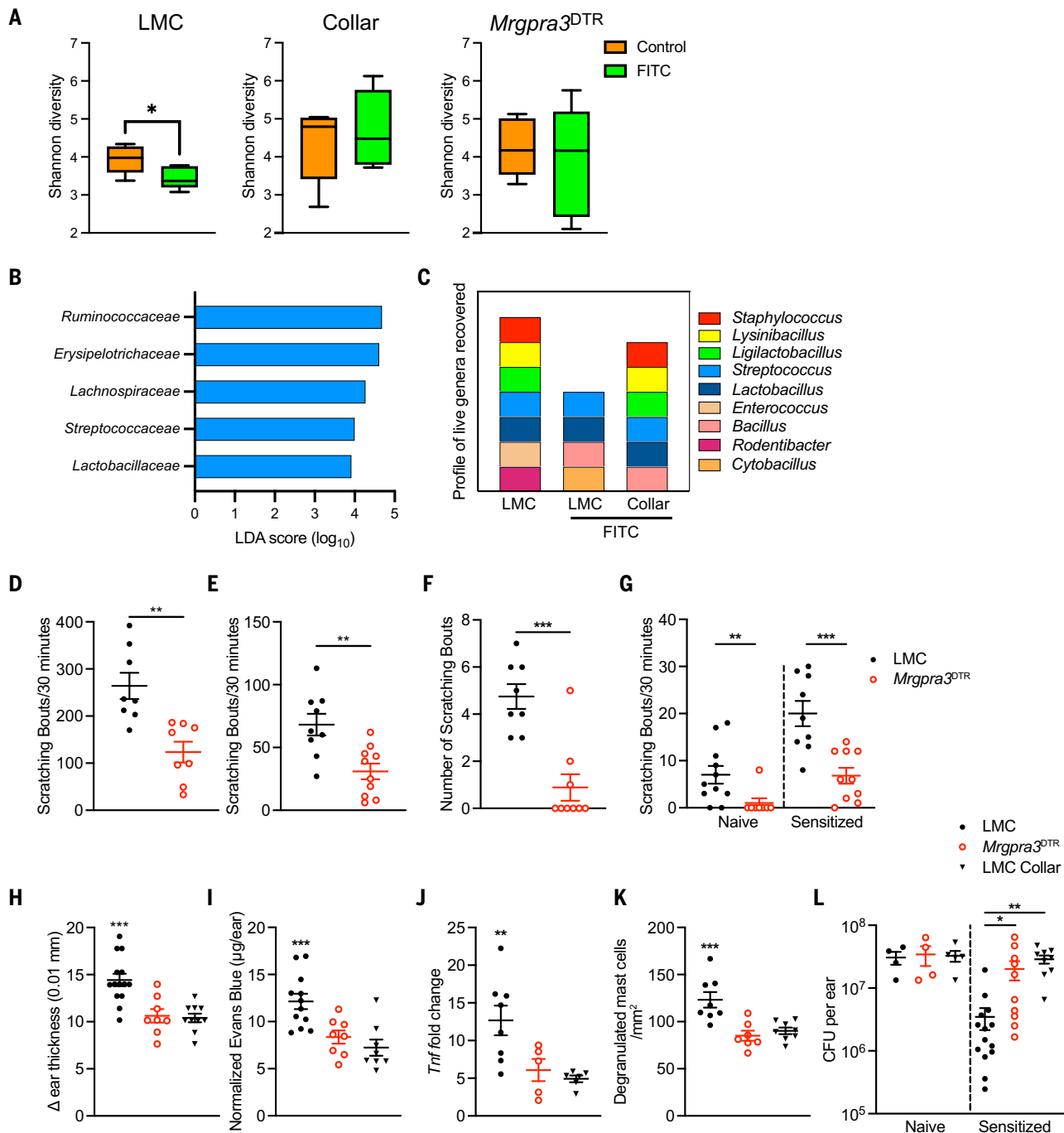


**Fig. 5. Scratching is required for *S. aureus*-induced scratching and host defense.**

(A and B) Shannon alpha diversity (A) and linear discriminant analysis (LDA) (B) of 16S rRNA-seq of the indicated groups. (C) The identity of live genera isolated from ear swabs obtained 24 hours after FITC challenge of the indicated group is shown (LMC and *Mrgpra3<sup>DTR</sup>*  $n = 5$ , collar  $n = 6$ ). (D) Scratching behavior over 30 min after i.d. nape injection of Staph V8 protease in DT-treated LMC and *Mrgpra3<sup>DTR</sup>* mice (LMC and *Mrgpra3<sup>DTR</sup>*  $n = 8$ ). (E) Scratching behavior over 30 min immediately after removal of occlusive *S. aureus* patch in DT-treated LMC (black circles) and *Mrgpra3<sup>DTR</sup>* (red circles) mice (LMC and *Mrgpra3<sup>DTR</sup>*  $n = 9$ ). (F) Ten hours after patch removal, allodynia was measured by a 0.04g von-Frey filament out of nine total stimuli in DT-treated LMC and *Mrgpra3<sup>DTR</sup>* mice (LMC  $n = 8$  and *Mrgpra3<sup>DTR</sup>*  $n = 9$ ). (G) Scratching behavior over 30 min after epicutaneous *S. aureus* ear infection in naïve and sensitized DT-treated LMC and *Mrgpra3<sup>DTR</sup>* mice (LMC  $n = 9$  to 11 and *Mrgpra3<sup>DTR</sup>*  $n = 8$  to 10). (H to K) Ear

thickness (H), quantification of EB extravasation (I), *Tnf* mRNA (J), and degranulated mast cells (K) quantified at 8 hours after epicutaneous *S. aureus* ear infection in sensitized DT-treated LMC, *Mrgpra3<sup>DTR</sup>*, and LMC collared (black triangles) mice (LMC  $n = 8$  to 14, *Mrgpra3<sup>DTR</sup>*  $n = 5$  to 8, collar  $n = 6$  to 10). (L) *S. aureus* ear CFU in DT-treated LMC, *Mrgpra3<sup>DTR</sup>*, and LMC collared mice that were either previously uninfected (naïve) or previously sensitized (LMC  $n = 4$  to 14, *Mrgpra3<sup>DTR</sup>*  $n = 4$  to 10, collar  $n = 5$  to 9). Tissue was harvested 24 hours after epicutaneous ear infection. Bars in (A) to (C) represent 25th to 75th percentiles, with whiskers extending to 10th and 90th percentiles. Horizontal bars indicate the medians. Individual data points in (D) to (L) represent data from a single animal, and bars show means  $\pm$  SEMs from three independent experiments. Significance was calculated using a Student's paired *t* test (A), a Mann-Whitney test [(D) to (G)], or a one-way ANOVA with multiple comparisons [(H) to (L)]. \* $P < 0.05$ ; \*\* $P < 0.01$ ; \*\*\* $P < 0.001$ .

that itch sensation in the FITC CHS model may be transduced by NP2.1 MrgprA3-expressing neurons that do not express TRPV1 and are not subjected to recombination in *Trpv1<sup>Cre</sup>* mice.

The requirement for both IgE and FcεRI in CHS responses has been well described (22, 39). The presence of increased IgE after a single hapten sensitization, however, was somewhat unexpected because IgE production often requires multiple immunizations and a longer time frame (62). Differential mast cell responses to MrgprB2 versus FcεRI activation have been reported based on the content of fused granules and which granule contents (e.g., histamine, proteases, and cytokines) are released (38, 47). Although FcεRI-mediated TNF release from mast cells has been well established, our work builds on these previous findings because we observe that the dual activation of both the FcεRI and MrgprB2 pathways can synergistically augment TNF release and increase neutrophil recruitment. We have focused only on TNF as a mast cell-derived effector cytokine owing to its well-defined role in mediating neutrophil recruitment and cutaneous inflammation in CHS (21–23). We recognize that MrgprB2 ligation may also affect mast cells activated through non-FcεRI-mediated mechanisms and that other mast cell-derived factors, such as CXCL1 and CXCL2, may also be affected (63). In addition, although we demonstrate the requirement of SP and MrgprB2 in our model, this may not be a direct effect, as SP may trigger the activation of keratinocytes to release other MrgprB2 ligands (64, 65).

We have demonstrated a cutaneous innate neuroimmune mechanism linking itch and scratching with adaptive allergic responses through mast cell activation. These findings illuminate a pharmacologically targetable mechanism by which scratching causes inflammation and reconciles the seemingly paradoxical role of scratching as a pathological process and evolutionary adaptation.

## Materials and methods

### Mice

C57BL/6J mice were purchased from Jackson Laboratory (Bar Harbor, ME). Mrgpra3Cre-gfp mice were generously provided by X. Dong (Johns Hopkins University, Baltimore, MD). Mrgpra3Cre-gfp mice were crossed with ROSA26iDTR (Jax Stock, no. 007900) mice to obtain *Mrgpra3<sup>DTR</sup>* mice. *Mrgprb2<sup>-/-</sup>* mice were kindly provided by B. McNeil (Northwestern University, Chicago, IL). *Tac1<sup>-/-</sup>* mice were purchased from Jackson Laboratory (Jax Stock, no. 004103). We crossed *Mcpt5Cre* (66) with *Rosa26iDTR* mice to obtain *Mcpt5<sup>DTR</sup>* mice. We crossed *TrpV1Cre* (Jax Stock, no. 017769) mice with *Rosa26-LSL-hm4Di-DREADD* (Jax Stock, no. 026219) mice to obtain *Trpv1<sup>hm4Di</sup>* mice. Experiments were performed on independent cohorts of male and female mice between the ages of 6 to 12 weeks.

FITC, Ox, PCA, and *S. aureus* experiments were conducted using female mice. Euthanasia was performed using CO<sub>2</sub>. All mice were maintained under specific pathogen-free conditions, and all animal experiments were approved by University of Pittsburgh Institutional Animal Care and Use Committee.

### DT-mediated neuronal ablation in MrgprA3<sup>DTR</sup> and Mcpt5<sup>DTR</sup> mice

To ablate MrgprA3-expressing neurons, 4-week-old MrgprA3-DTR and LMC mice were given six total doses of 300 ng DT (Fisher, NC972886) in 100 μl phosphate-buffered saline (PBS) (Fisher, 10010049) i.p. 3 days apart. In the model of neuronal ablation after hapten sensitization, mice were given two total doses of 600 ng DT in 100 μl PBS on days 3 and 6 postsensitization. To locally delete mast cells in *Mcpt5<sup>DTR</sup>* mice, we injected 120 ng DT i.d. at the ear pinna in FITC-sensitized mice 6 and 2 days before FITC challenge.

### Scratching behavior

Before behavioral recording, mice were habituated in clear plexiglass behavioral chambers for 30 to 60 min during the light cycle. The following pruritogens were injected in 20 μl PBS i.d. at the nape: chloroquine diphosphate (0.2 mg, Sigma, C6628), IL-31 (16 μg, Fisher, 210-31), and V8 protease (40 U, Worthington, LS003608). Scratching behavior was graded by a blinded observer.

### CHS

Mice were sensitized on day 0 by epicutaneous application of the following haptens: 100 μl of 0.5% FITC (Sigma-Aldrich F7250) in 1:1 acetone:dibutyl phthalate (Sigma-Aldrich 179973 and 524980), 100 μl of 2% Ox (4-Ethoxymethylene-2-phenyl-2-oxazolin-5-one, Sigma-Aldrich 862207) in 100% EtOH, or 25 μl of 0.5% DNFB (1-Fluoro-2,4-dinitrobenzene, Sigma-Aldrich D1529) in 4:1 acetone:olive oil (Sigma-Aldrich O1514) onto dry shaven abdominal skin. On day 5, baseline ear thickness was measured with a micrometer followed by challenge with 10 μl of 0.5% FITC to both sides of one ear, 10 μl of 1% Ox to the dorsal side of the ear, or 10 μl of 0.2% DNFB to both sides of one ear. Ear thickness was measured at the respective time points, with baseline ear thickness being subtracted to obtain the change in ear thickness. LMC collared mice were affixed with mouse Elizabethan collars (Kent Scientific EC201V) immediately after challenge. 80 μg BIBN4096 (Sigma SML2426) or vehicle [800 μl 5% dimethyl sulfoxide (DMSO)] was given i.p. 1 hour before FITC challenge and ear thickness was measured 24 hours postchallenge.

### Histology

Dissected mouse skin or DRG tissue were fixed in 4% paraformaldehyde (PFA) at 4°C for 2 hours,

cryoprotected in 25% sucrose in PBS for 24 hours, and embedded in optimal cutting temperature (OCT) compound at –80°C. DRG tissue was cut at 10 μm and skin tissue was cut at 6 μm and mounted onto Superfrost plus slides. Hematoxylin and eosin (H&E) histology was performed by UPMC Dermatopathology. For immunofluorescence, antibodies (below) were diluted in antibody diluting buffer [3% bovine serum albumin (BSA), 0.1% Tween20, in PBS] overnight and mounted using ProLong Gold antifade reagent with 4',6-diamidino-2-phenylindole (DAPI) (Thermo Fisher, P36935). Images were captured using the Keyence BZ-X810 fluorescent microscope (Keyence Corporation, Elmwood Park, NJ).

### Fluorescence in situ hybridization or RNAscope

RNAscope was carried out as previously described (67). Mice anesthetized with isoflurane were rapidly decapitated. DRGs were dissected within 5 min and embedded in OCT at –80°C. DRG tissue was cut at 15 μm, mounted directly onto Superfrost plus slides. RNAscope was performed according to the protocol using the RNAscope Multiplex Fluorescent v2 Assay (Advanced Cell Diagnostics, 323100). Probes used were Mm-Mrgpra3-C2 (ACDBio, 548161-C2) and mCitrine-O1-C3 (ACDBio, 1221581-C3).

### Flow cytometry

Single-cell suspensions were obtained as previously described (8). Whole skin was minced finely with scissors and resuspended in RPMI1640 (Gibco, MT10040CV) with 2.5 mg/ml collagenase XI (Sigma-Aldrich, C7657), 0.25 mg/ml hyaluronidase (Sigma-Aldrich, H3884), 0.1 mg/ml deoxyribonuclease (DNase) (Sigma-Aldrich, D5025), 0.01 M HEPES (Sigma-Aldrich, H0887), and 10% fetal bovine serum (FBS) (RnDSystems, S11550H) followed by incubation in a shaking incubator for 35 min at 37°C at 250 rpm. The digested tissues were then homogenized using a gentleMacs Dissociator (Miltenyi Biotec, 130-093-235). The resulting cells were filtered through a 40-mm cell strainer (BD Biosciences 352340). Antibodies (below) were diluted in staining media (2% Calf Serum, 5 mM EDTA, 0.04% Azide). After doublet and live/dead exclusion, cells were gated as follows: neutrophils, CD45+ CD11b+ Gr-1high; eosinophils CD45+ CD11b+ Gr-1-SiglecFhigh, dermal γδT cells, CD45+ CD3+TCRγδmid; CD4 T cells, CD45+ CD3+ TCRβ+ CD4+ CD8–; CD8 T cells, CD45+ CD3+ TCRβ+ CD4– CD8+. Data were analyzed using FlowJo software (TreeStar, Ashland, OR).

### Antibodies

Antibodies used include anti-GFP (Biolegend FM264G, AF488), TrpV1 (Alomone ACC-030), Sulforhodamine 101 conjugated Avidin (Sigma-Aldrich A2348), CD45.2 (Biolegend 104, BV421 or BV605), CD11b (Biolegend M1/70, AF700),

Gr-1 (Biolegend RB6-8C5, BV605), SiglecF (Biolegend E50-2440, PE), TCR $\beta$  (Biolegend H57-597, PE-Texas Red), TCR $\gamma\delta$  (Biolegend GL3, AF647), CD4 (Biolegend RM4-5, BV421), CD8a (Biolegend 53-6.7, BUV737), and CD3 $\epsilon$  (Biolegend 17A2, PE).

#### RNA

Tissue was homogenized using the Navy RINO Lysis Kit (Next Advance, NAVYR5) RNA was isolated from whole skin using Trizol (Sigma-Aldrich, T9424) following the manufacturer's protocol. RNA to cDNA conversion was performed using a High Capacity cDNA Reverse Transcription Kit (Applied Biosystems, 4368813). cDNA was analyzed using TaqMan Gene Expression assays (Tnf assay ID: Mm00443258\_m1, Tslp assay ID: Mm01157588\_m1). CT values are normalized to gene expression levels in untreated LMC tissue.

#### In vivo mast cell assays

For in vivo activation of mast cells by MrgprB2 ligation, ear thickness was measured before injection of 200 ng Compound 48/80 (Sigma-Aldrich, C2313) or 1.2  $\mu$ g SP (Tocris, NC2226616) in 20  $\mu$ l PBS into the ear pinna with an insulin needle. EB extravasation was carried out as previously described (18, 68). For FITC and Ox challenge, mice were anesthetized using isoflurane and 1.25 mg EB (Sigma-Aldrich, E2129) in 50  $\mu$ l PBS was given retro-orbitally 15 min before hapten challenge. For the in vivo activation of mast cells by Fc $\epsilon$ RI cross-linking, 20 ng dinitrophenyl-specific IgE (Sigma-Aldrich, D8406) in 20  $\mu$ l PBS was injected i.d. in the ear pinna. 20 hours later, mice were anesthetized and 0.625 mg EB in 50  $\mu$ l PBS was administered retro-orbitally. 15 min later, baseline ear thickness was measured and 2  $\mu$ g DNP (Sigma-Aldrich, A6661) in 20  $\mu$ l PBS was applied to the ear pinna i.d. For QWF experiments, vehicle control or QWF (Tocris, 66-425), prepared as previously described (69), was mixed with DNP and injected. EB was extracted by incubation in formamide (Sigma-Aldrich, D4551) overnight at 37°C, and the OD was read at 650 nm using a spectrophotometer (Biotek, EPOCH) and analyzed using Gen5 software. Normalized EB was calculated by subtracting EB in untreated tissue.

#### Serum collection and IgE enzyme-linked immunosorbent assay (ELISA)

Untreated and LMC and MrgprA3-DTR mice were bled 10 hours after FITC, Ox, and DNFB challenge. *S. aureus*-immunized LMC and MrgprA3-DTR mice were bled 14 days after epicutaneous immunization. Blood samples were then incubated at room temperature for 30 min and centrifuged at 1500g for 10 min. Serum was collected and stored at -20°C. Serum was diluted 5x in 10% FBS and total IgE levels in serum were quantified using a

mouse IgE ELISA (BD Biosciences, 555248) according to the manufacturer's protocol.

#### Cytokine protein expression

Tissue was homogenized in 500  $\mu$ l Cell extraction buffer (Invitrogen, FNN0011) supplemented with phenylmethylsulfonyl fluoride (PMSF) (Sigma-Aldrich, 52332) and protease inhibitor (Sigma-Aldrich, P2714) according to the manufacturer's recommendation. Tissue homogenates were centrifuged for 10 min at 7500 rpm. TNF and IL-33 levels in supernatant were quantified using a bead-based LEGENDplex immunoassay (Biolegend, 740134) according to the manufacturer's protocol. Samples were analyzed on LSRFortessa flow cytometers (Becton Dickinson, Franklin Lakes, NJ). Data were analyzed using LEGENDplex analysis software. TSLP levels in supernatant were quantified using a TSLP ELISA (R&D Systems, DY555) according to the manufacturer's protocol.

#### Chemogenetic inhibition of nociceptors

To inhibit TrpV1-expressing nociceptors, CNO dihydrochloride (Tocris, 6329) was injected i.p. at 1 mg/kg. To measure thermal nociception, we used a plantar testing apparatus (IITC, 390G). Mice treated with CNO were habituated for 1 hour in individual clear Plexiglas (acrylic plastic) chambers. A focused light beam was then applied to the plantar surface of the hindpaw. The mean of three paw withdrawal latencies was determined after measurements at baseline and 1, 3, 5, 7, 9, 11, and 13 hours after CNO injection. In PCA and FITC experiments in which TrpV1<sup>hM4Di</sup> mice were used, CNO was given 1 hour before challenge.

#### Capsaicin activation of nociceptors

For PCA experiments, capsaicin (Sigma-Aldrich, M2028) was mixed with 2  $\mu$ g DNP at a concentration of 0.5  $\mu$ g in 10% DMSO (Sigma-Aldrich, D2650) and injected i.d. in the ear pinna. Mice in the PCA control and collared groups were treated with 2  $\mu$ g DNP in 10% DMSO injected i.d. in the ear pinna. For FITC experiments, 3.05  $\mu$ g capsaicin in 10  $\mu$ l 100% EtOH was applied topically to both sides of one ear 10 min after FITC challenge. Mice in the FITC control and collared groups were treated with 10  $\mu$ l 100% topical EtOH applied topically to both sides of one ear 10 min after FITC challenge. All capsaicin-treated mice were then affixed with mouse Elizabethan collars.

#### Detection of cutaneous SP

Mice sensitized with DNP-IgE were either challenged with an i.d. capsaicin or DNP injection. Within 30 min postchallenge, whole ears were harvested, split into dorsal and ventral halves, then placed in a 24-well plate containing 1 ml Dulbecco's minimum essential medium (DMEM), which was then placed in a shaking incubator

set at 32°C and 150 rpm for 45 min. Bath supernatants were then collected and analyzed for SP levels using the SP ELISA kit (Cayman chemical).

#### Mast cell culture

Peritoneal cells isolated from 6- to 10-week-old C57BL/6 female mice were cultured in RPMI1640 medium supplemented with 10% heat-inactivated fetal bovine serum (RnDSystems, S11550H), 20 mM HEPES (Sigma-Aldrich, H0887), 1 mM sodium pyruvate (Gibco, 11360070), 1x non-essential amino acids (Corning, MT25-025-CI), 50  $\mu$ M 2-mercaptoethanol (Sigma-Aldrich, M3148), 50  $\mu$ g/ml penicillin/streptomycin (Gibco, 15140122), 4 mM L-glutamine (Corning, MT25-005-CI), and 25 ng/ml recombinant mouse IL-3 (PeproTech, 21313), and 15 ng/ml stem cell factor (PeproTech, 250-03). The cells were maintained at a concentration of  $0.5 \times 10^6$  to  $1 \times 10^6$  cells/ml with weekly changes of the medium. After 3 weeks of culturing, the cell population purity was confirmed by flow cytometry, with more than 95% of cells being mast cells. Mast cells were then treated with 1 ng/ml DNP-specific IgE. 16 hours later, the cells were then washed and cultured in Tyrode's buffer with varying concentrations of DNP (0, 1, 10, 100, and 1000 ng/ml). After a 30-min stimulation at 37°C, varying 48/80 or SP solutions in Tyrode's buffer was added to a final concentration of 0, 5, 20, and 50  $\mu$ g/ml (48/80) or 0, 100, 250, and 1000  $\mu$ g/ml (SP). Six hours after DNP administration, the supernatant was harvested and stored at -80°C. TNF was measured using a bead-based LegendPlex as mentioned above.  $\beta$ -hex was detected as previously described (70), with optical density (OD) being read at 405 nm using a spectrophotometer.

#### *S. aureus* infection

Methicillin-resistant *S. aureus* strain USA300 (ATCC, fpr3757) was grown in BD Bacto Tryptic Soy Broth (TSB) (Fisher, 211825) media overnight at 37°C. The overnight culture was then diluted 1:200 and grown for 2 to 3 hours in TSB and thoroughly washed in sterile PBS. Bacteria were then resuspended in sterile PBS at the desired concentration. *S. aureus* flank infection was carried out as previously described (30). Two days before infection, mice back fur was removed using electric clippers and chemical depilation. Mice were infected with  $10^7$  CFU USA in 100  $\mu$ l sterile PBS on a 1-cm<sup>2</sup> gauze pad under a Tegaderm patch. The patched area was then wrapped twice using sterile adhesive bandages. Five days after epicutaneous immunization, bandages and patches were removed and passive scratching behavior was recorded after a 30-min habituation period. Nine hours after patch removal, mice were habituated in allonknesis chambers for 1 hour. The skin formerly under the patch of each mouse was stimulated with a 0.04g Von Frey

filament three times in a row. The triple stimulation was repeated two more times resulting in nine total stimulations. *S. aureus* ear infection was carried out as previously described (25). The right ears of anesthetized mice were then cleaned using 70% isopropanol and allowed to dry.  $10^9$  CFU in 10  $\mu$ l sterile PBS was then pipetted on to the tip of a sterile plastic allergy needle (Morrow Brown Allergy Diagnostics, M-952308-4075). After baseline ear thickness measurement, the ventral side of the right ear was then pricked eight times with the staph-coated needle. Eight hours after infection, ear thickness was measured and tissue was collected for RNA, EB, and histological analysis. 24 hours after infection, the infected ear was cleaned with 70% isopropanol and homogenized in RINO tubes before dilution and plating on TSB plates. After an overnight incubation at 37°C, colonies were then quantified.

#### Analysis of the cutaneous microbiome

LMC and *Mrgpra3*<sup>DTR</sup> mice were cohoused until FITC challenge. 24 hours after FITC challenge, ears were swabbed equally on the ventral and dorsal sides using sterile Q-tips presoaked with sterile PBS. Swabs were submerged in an aliquot of sterile PBS until processing for culturomics (see below). Whole ears were then harvested and snap frozen using liquid nitrogen. Whole ear samples were processed for 16S rRNA-seq and analysis, which was performed by Zymo Research's Microbiome Sequencing Services, Irving, CA as previously described (71).

#### Culturomics

Sterile ear swabs were incubated in PBS at room temperature for 30 min, and then samples were aliquoted into four different bacteriological growth media for pre-expansion of bacterial communities: Brain Heart Infusion Broth (Fisher Scientific, CM1135B) supplemented with 5% sheep's blood (Fisher Defibrinated Blood, 50-863-753) (BHI + 5%), DeMann Rosa Sharpe (Fisher Scientific, DF0881-17-5) (MRS) Broth, Reinforced Clostridial (Fisher Scientific, cat. no. OXCM0149B) (RCL) Broth, and Cooked Meat (Fisher BD, cat. no. 226730) (CMM) Broth. Culture broths were incubated for 48 hours aerobically (37°C). Cultures were then streaked for single colony isolation across six different agars (Fisher BD, DF0140-01-0) as follows: BHI + 5% broth culture was streaked on BHI + 5% agar, Chocolate Agar (Fisher Scientific, R01300), and Tryptic Soy (Fisher Scientific, DF0370-17-3) Agar; RCL broth culture was streaked on RCL agar; CMM broth culture was streaked on CMM agar; and MRS broth culture was streaked on MRS agar. Agar plates were incubated aerobically at 37°C for 48 hours. Single colonies were then picked from agar plates for identification by 16S rRNA single-colony sequencing.

#### Bacterial colony identification

Bacterial colonies were identified as previously described (58, 72). In brief, grown colonies were picked with sterile pipette tips and stored at -80°C until analysis. On the day of analysis, picked bacterial colonies were thawed at room temperature, resuspended with 20  $\mu$ l of sterile ATE buffer (Qiagen) and lysed at 95°C for 10 min. Samples were subsequently cooled down to 4°C and then the DNA (2  $\mu$ l) was used as template DNA in polymerase chain reaction (PCR) reactions amplifying the 16S rRNA gene using universal bacterial 16S rRNA primers (27F, 50-AGAGTTTGATCMTGGCTCAG-30 and 1525R, 50-AAGGAGGTGATCCAGCC-30) with reaction conditions: 95°C for 5 min followed by 35 cycles of 95°C for 30 s, 55°C for 30 s, 72°C for 2 min, and then 72°C for 20 min. The amplification product (8  $\mu$ l) was incubated with 2  $\mu$ l ExoSAP-ITTM (Thermo Fisher, 78201) for 37°C for 15 min, followed by 80°C for 15 min. Amplicons were sequenced by capillary sequencing, and the resulting sequences were analyzed using BLASTN and the 16S rRNA sequences NCBI database for species identification.

#### REFERENCES AND NOTES

- F. Cevikbas, E. A. Lerner, Physiology and Pathophysiology of Itch. *Physiol. Rev.* **100**, 945–982 (2020). doi: [10.1152/physrev.00017.2019](https://doi.org/10.1152/physrev.00017.2019); pmid: [31869278](https://pubmed.ncbi.nlm.nih.gov/31869278/)
- S. Ständer, Atopic Dermatitis. *N. Engl. J. Med.* **384**, 1136–1143 (2021). doi: [10.1056/NEJMra2023911](https://doi.org/10.1056/NEJMra2023911); pmid: [33761208](https://pubmed.ncbi.nlm.nih.gov/33761208/)
- M. N. Balki, A. V. Apkarian, Nociception, Pain, Negative Moods, and Behavior Selection. *Neuron* **87**, 474–491 (2015). doi: [10.1016/j.neuron.2015.06.005](https://doi.org/10.1016/j.neuron.2015.06.005); pmid: [26247858](https://pubmed.ncbi.nlm.nih.gov/26247858/)
- L. K. Oetjen et al., Sensory Neurons Co-opt Classical Immune Signaling Pathways to Mediate Chronic Itch. *Cell* **171**, 217–228.e13 (2017). doi: [10.1016/j.cell.2017.08.006](https://doi.org/10.1016/j.cell.2017.08.006); pmid: [28890086](https://pubmed.ncbi.nlm.nih.gov/28890086/)
- S. M. Langan, A. D. Irvine, S. Weidinger, Atopic dermatitis. *Lancet* **396**, 345–360 (2020). doi: [10.1016/S0140-6736\(20\)31286-1](https://doi.org/10.1016/S0140-6736(20)31286-1); pmid: [32738956](https://pubmed.ncbi.nlm.nih.gov/32738956/)
- I. M. Chiu et al., Bacteria activate sensory neurons that modulate pain and inflammation. *Nature* **501**, 52–57 (2013). doi: [10.1038/nature12479](https://doi.org/10.1038/nature12479); pmid: [23965627](https://pubmed.ncbi.nlm.nih.gov/23965627/)
- F. A. Pinho-Ribeiro, W. A. Verri Jr., I. M. Chiu, Nociceptor Sensory Neuron-Immune Interactions in Pain and Inflammation. *Trends Immunol.* **38**, 5–19 (2017). doi: [10.1016/j.it.2016.10.001](https://doi.org/10.1016/j.it.2016.10.001); pmid: [27793571](https://pubmed.ncbi.nlm.nih.gov/27793571/)
- S. W. Kashem et al., Nociceptive Sensory Fibers Drive Interleukin-23 Production from CD301b<sup>+</sup> Dermal Dendritic Cells and Drive Protective Cutaneous Immunity. *Immunity* **43**, 515–526 (2015). doi: [10.1016/j.immuni.2015.08.016](https://doi.org/10.1016/j.immuni.2015.08.016); pmid: [26377898](https://pubmed.ncbi.nlm.nih.gov/26377898/)
- J. A. Cohen et al., Cutaneous TRPV1<sup>+</sup> Neurons Trigger Protective Innate Type 17 Anticipatory Immunity. *Cell* **178**, 919–932.e14 (2019). doi: [10.1016/j.cell.2019.06.022](https://doi.org/10.1016/j.cell.2019.06.022); pmid: [31353219](https://pubmed.ncbi.nlm.nih.gov/31353219/)
- F. Wang, B. S. Kim, Itch: A Paradigm of Neuroimmune Crosstalk. *Immunity* **52**, 753–766 (2020). doi: [10.1016/j.immuni.2020.04.008](https://doi.org/10.1016/j.immuni.2020.04.008); pmid: [32433948](https://pubmed.ncbi.nlm.nih.gov/32433948/)
- N. Serhan, N. Cenac, L. Basso, N. Gaudenzi, Mas-related G protein-coupled receptors (Mrgprs) - Key regulators of neuroimmune interactions. *Neurosci. Lett.* **749**, 135724 (2021). doi: [10.1016/j.neulet.2021.135724](https://doi.org/10.1016/j.neulet.2021.135724); pmid: [33600909](https://pubmed.ncbi.nlm.nih.gov/33600909/)
- D. Usoskin et al., Unbiased classification of sensory neuron types by large-scale single-cell RNA sequencing. *Nat. Neurosci.* **18**, 145–153 (2015). doi: [10.1038/nn.3881](https://doi.org/10.1038/nn.3881); pmid: [25420068](https://pubmed.ncbi.nlm.nih.gov/25420068/)
- L. Han et al., A subpopulation of nociceptors specifically linked to itch. *Nat. Neurosci.* **16**, 174–182 (2013). doi: [10.1038/nn.3289](https://doi.org/10.1038/nn.3289); pmid: [23263443](https://pubmed.ncbi.nlm.nih.gov/23263443/)
- A. W. Liu, J. E. Gillis, T. L. Sumpter, D. H. Kaplan, Neuroimmune interactions in atopic and allergic contact dermatitis. *J. Allergy Clin. Immunol.* **151**, 1169–1177 (2023). doi: [10.1016/j.jaci.2023.03.013](https://doi.org/10.1016/j.jaci.2023.03.013); pmid: [37149370](https://pubmed.ncbi.nlm.nih.gov/37149370/)
- S. R. Wilson et al., The epithelial cell-derived atopic dermatitis cytokine TSLP activates neurons to induce itch. *Cell* **155**,

- 285–295 (2013). doi: [10.1016/j.cell.2013.08.057](https://doi.org/10.1016/j.cell.2013.08.057); pmid: [24094650](https://pubmed.ncbi.nlm.nih.gov/24094650/)
- X. Dong, X. Dong, Peripheral and Central Mechanisms of Itch. *Neuron* **98**, 482–494 (2018). doi: [10.1016/j.neuron.2018.03.023](https://doi.org/10.1016/j.neuron.2018.03.023); pmid: [29723501](https://pubmed.ncbi.nlm.nih.gov/29723501/)
- S. J. Galli, M. Tsai, IgE and mast cells in allergic disease. *Nat. Med.* **18**, 693–704 (2012). doi: [10.1038/nm.2755](https://doi.org/10.1038/nm.2755); pmid: [22561833](https://pubmed.ncbi.nlm.nih.gov/22561833/)
- B. D. McNeil et al., Identification of a mast-cell-specific receptor crucial for pseudo-allergic drug reactions. *Nature* **519**, 237–241 (2015). doi: [10.1038/nature14022](https://doi.org/10.1038/nature14022); pmid: [25517090](https://pubmed.ncbi.nlm.nih.gov/25517090/)
- S. N. Abraham, A. L. St. John, Mast cell-orchestrated immunity to pathogens. *Nat. Rev. Immunol.* **10**, 440–452 (2010). doi: [10.1038/nri2782](https://doi.org/10.1038/nri2782); pmid: [20498670](https://pubmed.ncbi.nlm.nih.gov/20498670/)
- N. Gaudenzi, L. Basso, Mast cell-neuron axis in allergy. *Curr. Opin. Immunol.* **77**, 102213 (2022). doi: [10.1016/j.coi.2022.102213](https://doi.org/10.1016/j.coi.2022.102213); pmid: [35605523](https://pubmed.ncbi.nlm.nih.gov/35605523/)
- J. Dudeck et al., Directional mast cell degranulation of tumor necrosis factor into blood vessels primes neutrophil extravasation. *Immunity* **54**, 468–483.e5 (2021). doi: [10.1016/j.immuni.2020.12.017](https://doi.org/10.1016/j.immuni.2020.12.017); pmid: [33484643](https://pubmed.ncbi.nlm.nih.gov/33484643/)
- P. J. Bryce et al., Immune sensitization in the skin is enhanced by antigen-independent effects of IgE. *Immunity* **20**, 381–392 (2004). doi: [10.1016/S1074-7613\(04\)00080-9](https://doi.org/10.1016/S1074-7613(04)00080-9); pmid: [15084268](https://pubmed.ncbi.nlm.nih.gov/15084268/)
- K. Takeshita, T. Yamasaki, S. Akira, F. Gantner, K. B. Bacon, Essential role of MHC II-independent CD4<sup>+</sup> T cells, IL-4 and STAT6 in contact hypersensitivity induced by fluorescein isothiocyanate in the mouse. *Int. Immunol.* **16**, 685–695 (2004). doi: [10.1093/intimm/dxh073](https://doi.org/10.1093/intimm/dxh073); pmid: [15096484](https://pubmed.ncbi.nlm.nih.gov/15096484/)
- M. Arifuzzaman et al., MRGPR-mediated activation of local mast cells clears cutaneous bacterial infection and protects against reinfection. *Sci. Adv.* **5**, eaav0216 (2019). doi: [10.1126/sciadv.aav0216](https://doi.org/10.1126/sciadv.aav0216); pmid: [30613778](https://pubmed.ncbi.nlm.nih.gov/30613778/)
- P. Starkl et al., IgE Effector Mechanisms, in Concert with Mast Cells, Contribute to Acquired Host Defense against *Staphylococcus aureus*. *Immunity* **53**, 1333 (2020). doi: [10.1016/j.immuni.2020.11.012](https://doi.org/10.1016/j.immuni.2020.11.012); pmid: [33326769](https://pubmed.ncbi.nlm.nih.gov/33326769/)
- C. M. Rocha-de-Souza, B. Berent-Maaz, D. Mankuta, A. E. Moses, F. Levi-Schaffer, Human mast cell activation by *Staphylococcus aureus*: Interleukin-8 and tumor necrosis factor alpha release and the role of Toll-like receptor 2 and CD48 molecules. *Infect. Immun.* **76**, 4489–4497 (2008). doi: [10.1128/IAI.00270-08](https://doi.org/10.1128/IAI.00270-08); pmid: [18644875](https://pubmed.ncbi.nlm.nih.gov/18644875/)
- L. A. Pogorzala, S. K. Mishra, M. A. Hoon, The cellular code for mammalian thermosensation. *J. Neurosci.* **33**, 5533–5541 (2013). doi: [10.1523/JNEUROSCI.5788-12.2013](https://doi.org/10.1523/JNEUROSCI.5788-12.2013); pmid: [23536068](https://pubmed.ncbi.nlm.nih.gov/23536068/)
- A. Zeisel et al., Molecular Architecture of the Mouse Nervous System. *Cell* **174**, 999–1014.e22 (2018). doi: [10.1016/j.cell.2018.06.021](https://doi.org/10.1016/j.cell.2018.06.021); pmid: [30096314](https://pubmed.ncbi.nlm.nih.gov/30096314/)
- N. Sharma et al., The emergence of transcriptional identity in somatosensory neurons. *Nature* **577**, 392–398 (2020). doi: [10.1038/s41586-019-1900-1](https://doi.org/10.1038/s41586-019-1900-1); pmid: [31915380](https://pubmed.ncbi.nlm.nih.gov/31915380/)
- L. Deng et al., *S. aureus* drives itch and scratch-induced skin damage through a V8 protease-PAR1 axis. *Cell* **186**, 5375–5393.e25 (2023). doi: [10.1016/j.cell.2023.10.019](https://doi.org/10.1016/j.cell.2023.10.019); pmid: [37995657](https://pubmed.ncbi.nlm.nih.gov/37995657/)
- B. K. Wershil, Z. S. Wang, J. R. Gordon, S. J. Galli, Recruitment of neutrophils during IgE-dependent cutaneous late phase reactions in the mouse is mast cell-dependent. Partial inhibition of the reaction with antiserum against tumor necrosis factor- $\alpha$ . *J. Clin. Invest.* **87**, 446–453 (1991). doi: [10.1172/JCI115016](https://doi.org/10.1172/JCI115016); pmid: [1991831](https://pubmed.ncbi.nlm.nih.gov/1991831/)
- T. Biedermann et al., Mast cells control neutrophil recruitment during T cell-mediated delayed-type hypersensitivity reactions through tumor necrosis factor and macrophage inflammatory protein 2. *J. Exp. Med.* **192**, 1441–1452 (2000). doi: [10.1084/jem.192.10.1441](https://doi.org/10.1084/jem.192.10.1441); pmid: [11085746](https://pubmed.ncbi.nlm.nih.gov/11085746/)
- M. K. Oyoshi, R. P. Larson, S. F. Ziegler, R. S. Geha, Mechanical injury polarizes skin dendritic cells to elicit a Th2 response by inducing cutaneous thymic stromal lymphopoietin expression. *J. Allergy Clin. Immunol.* **126**, 976–984.e5 (2010). doi: [10.1016/j.jaci.2010.08.041](https://doi.org/10.1016/j.jaci.2010.08.041); pmid: [21050944](https://pubmed.ncbi.nlm.nih.gov/21050944/)
- J. M. Leyva-Castillo, P. Hener, H. Jiang, M. Li, TSLP produced by keratinocytes promotes allergen sensitization through skin and thereby triggers atopic march in mice. *J. Invest. Dermatol.* **133**, 154–163 (2013). doi: [10.1038/jid.2012.239](https://doi.org/10.1038/jid.2012.239); pmid: [22832486](https://pubmed.ncbi.nlm.nih.gov/22832486/)
- R. Malaviya, T. Ikeda, E. Ross, S. N. Abraham, Mast cell modulation of neutrophil influx and bacterial clearance at sites of infection through TNF- $\alpha$ . *Nature* **381**, 77–80 (1996). doi: [10.1038/381077a0](https://doi.org/10.1038/381077a0); pmid: [8609993](https://pubmed.ncbi.nlm.nih.gov/8609993/)

36. H. Suto *et al.*, Mast cell-associated TNF promotes dendritic cell migration. *J. Immunol.* **176**, 4102–4112 (2006). doi: [10.4049/jimmunol.176.7.4102](https://doi.org/10.4049/jimmunol.176.7.4102); pmid: [16547246](https://pubmed.ncbi.nlm.nih.gov/16547246/)
37. A. Dudeck *et al.*, Mast cells are key promoters of contact allergy that mediate the adjuvant effects of haptens. *Immunity* **34**, 973–984 (2011). doi: [10.1016/j.immuni.2011.03.028](https://doi.org/10.1016/j.immuni.2011.03.028); pmid: [21703544](https://pubmed.ncbi.nlm.nih.gov/21703544/)
38. N. Gaudenzio *et al.*, Different activation signals induce distinct mast cell degranulation strategies. *J. Clin. Invest.* **126**, 3981–3998 (2016). doi: [10.1172/JCI85538](https://doi.org/10.1172/JCI85538); pmid: [27643442](https://pubmed.ncbi.nlm.nih.gov/27643442/)
39. M. Kobayashi *et al.*, Abrogation of high-affinity IgE receptor-mediated mast cell activation at the effector phase prevents contact hypersensitivity to oxazolone. *J. Invest. Dermatol.* **130**, 725–731 (2010). doi: [10.1038/jid.2009.289](https://doi.org/10.1038/jid.2009.289); pmid: [19741711](https://pubmed.ncbi.nlm.nih.gov/19741711/)
40. A. Takamori *et al.*, IL-31 is crucial for induction of pruritus, but not inflammation, in contact hypersensitivity. *Sci. Rep.* **8**, 6639 (2018). doi: [10.1038/s41598-018-25094-4](https://doi.org/10.1038/s41598-018-25094-4); pmid: [29703903](https://pubmed.ncbi.nlm.nih.gov/29703903/)
41. H. Nagai *et al.*, Different role of IL-4 in the onset of hapten-induced contact hypersensitivity in BALB/c and C57BL/6 mice. *Br. J. Pharmacol.* **129**, 299–306 (2000). doi: [10.1038/sj.bjp.0703054](https://doi.org/10.1038/sj.bjp.0703054); pmid: [10694236](https://pubmed.ncbi.nlm.nih.gov/10694236/)
42. N.-R. Han *et al.*, TSLP induces mast cell development and aggravates allergic reactions through the activation of MDM2 and STAT6. *J. Invest. Dermatol.* **134**, 2521–2530 (2014). doi: [10.1038/jid.2014.198](https://doi.org/10.1038/jid.2014.198); pmid: [24751726](https://pubmed.ncbi.nlm.nih.gov/24751726/)
43. R. Saluja, A. Zoltowska, M. E. Ketelaar, G. Nilsson, IL-33 and Thymic Stromal Lymphopoietin in mast cell functions. *Eur. J. Pharmacol.* **778**, 68–76 (2016). doi: [10.1016/j.ejphar.2015.04.047](https://doi.org/10.1016/j.ejphar.2015.04.047); pmid: [26051792](https://pubmed.ncbi.nlm.nih.gov/26051792/)
44. C. Galand *et al.*, IL-33 promotes food anaphylaxis in epicutaneously sensitized mice by targeting mast cells. *J. Allergy Clin. Immunol.* **138**, 1356–1366 (2016). doi: [10.1016/j.jaci.2016.03.056](https://doi.org/10.1016/j.jaci.2016.03.056); pmid: [27372570](https://pubmed.ncbi.nlm.nih.gov/27372570/)
45. A. M. Trier *et al.*, IL-33 potentiates histaminergic itch. *J. Allergy Clin. Immunol.* **153**, 852–859.e3 (2024). doi: [10.1016/j.jaci.2023.08.038](https://doi.org/10.1016/j.jaci.2023.08.038); pmid: [37984799](https://pubmed.ncbi.nlm.nih.gov/37984799/)
46. M. Tauber *et al.*, Landscape of mast cell populations across organs in mice and humans. *J. Exp. Med.* **220**, e20230570 (2023). doi: [10.1084/jem.20230570](https://doi.org/10.1084/jem.20230570); pmid: [37462672](https://pubmed.ncbi.nlm.nih.gov/37462672/)
47. J. Meixiong *et al.*, Activation of Mast-Cell-Expressed Mas-Related G-Protein-Coupled Receptors Drives Non-histaminergic Itch. *Immunity* **50**, 1163–1171.e5 (2019). doi: [10.1016/j.immuni.2019.03.013](https://doi.org/10.1016/j.immuni.2019.03.013); pmid: [31027996](https://pubmed.ncbi.nlm.nih.gov/31027996/)
48. V. Tsvilovskyy, A. Solis-Lopez, K. Öhlenschläger, M. Freichel, Isolation of Peritoneum-derived Mast Cells and Their Functional Characterization with Ca<sup>2+</sup>-imaging and Degranulation Assays. *J. Vis. Exp.* **137**, e57222 (2018). doi: [10.3791/57222](https://doi.org/10.3791/57222); pmid: [30035759](https://pubmed.ncbi.nlm.nih.gov/30035759/)
49. N. Serhan *et al.*, House dust mites activate nociceptor-mast cell clusters to drive type 2 skin inflammation. *Nat. Immunol.* **20**, 1435–1443 (2019). doi: [10.1038/s41590-019-0493-z](https://doi.org/10.1038/s41590-019-0493-z); pmid: [31591569](https://pubmed.ncbi.nlm.nih.gov/31591569/)
50. C. Perner *et al.*, Substance P Release by Sensory Neurons Triggers Dendritic Cell Migration and Initiates the Type-2 Immune Response to Allergens. *Immunity* **53**, 1063–1077.e7 (2020). doi: [10.1016/j.immuni.2020.10.001](https://doi.org/10.1016/j.immuni.2020.10.001); pmid: [33098765](https://pubmed.ncbi.nlm.nih.gov/33098765/)
51. J. Yamaoka, S. Kawana, Rapid changes in substance P signaling and neutral endopeptidase induced by skin-itching stimulation in mice. *J. Dermatol. Sci.* **48**, 123–132 (2007). doi: [10.1016/j.jdermsci.2007.06.007](https://doi.org/10.1016/j.jdermsci.2007.06.007); pmid: [17692507](https://pubmed.ncbi.nlm.nih.gov/17692507/)
52. J. A. Geoghegan, A. D. Irvine, T. J. Foster, *Staphylococcus aureus* and Atopic Dermatitis: A Complex and Evolving Relationship. *Trends Microbiol.* **26**, 484–497 (2018). doi: [10.1016/j.tim.2017.11.008](https://doi.org/10.1016/j.tim.2017.11.008); pmid: [29233606](https://pubmed.ncbi.nlm.nih.gov/29233606/)
53. J. J. Leyden, R. R. Marples, A. M. Kligman, *Staphylococcus aureus* in the lesions of atopic dermatitis. *Br. J. Dermatol.* **90**, 525–530 (1974). doi: [10.1111/j.1365-2133.1974.tb06447.x](https://doi.org/10.1111/j.1365-2133.1974.tb06447.x); pmid: [4601016](https://pubmed.ncbi.nlm.nih.gov/4601016/)
54. T. Kobayashi *et al.*, Dysbiosis and *Staphylococcus aureus* Colonization Drives Inflammation in Atopic Dermatitis. *Immunity* **42**, 756–766 (2015). doi: [10.1016/j.immuni.2015.03.014](https://doi.org/10.1016/j.immuni.2015.03.014); pmid: [25902485](https://pubmed.ncbi.nlm.nih.gov/25902485/)
55. H. H. Kong *et al.*, Temporal shifts in the skin microbiome associated with disease flares and treatment in children with atopic dermatitis. *Genome Res.* **22**, 850–859 (2012). doi: [10.1101/gr.131029.111](https://doi.org/10.1101/gr.131029.111); pmid: [22310478](https://pubmed.ncbi.nlm.nih.gov/22310478/)
56. B. Shi *et al.*, The skin microbiome is different in pediatric versus adult atopic dermatitis. *J. Allergy Clin. Immunol.* **138**, 1233–1236 (2016). doi: [10.1016/j.jaci.2016.04.053](https://doi.org/10.1016/j.jaci.2016.04.053); pmid: [27474122](https://pubmed.ncbi.nlm.nih.gov/27474122/)
57. L. F. Koh, R. Y. Ong, J. E. Common, Skin microbiome of atopic dermatitis. *Allergol. Int.* **71**, 31–39 (2022). doi: [10.1016/j.alit.2021.11.001](https://doi.org/10.1016/j.alit.2021.11.001); pmid: [34838450](https://pubmed.ncbi.nlm.nih.gov/34838450/)
58. M. J. Bender *et al.*, Dietary tryptophan metabolite released by intratumoral *Lactobacillus reuteri* facilitates immune checkpoint inhibitor treatment. *Cell* **186**, 1846–1862.e26 (2023). doi: [10.1016/j.cell.2023.03.011](https://doi.org/10.1016/j.cell.2023.03.011); pmid: [37028428](https://pubmed.ncbi.nlm.nih.gov/37028428/)
59. H. Liu *et al.*, *Staphylococcus aureus* Epicutaneous Exposure Drives Skin Inflammation via IL-36-Mediated T Cell Responses. *Cell Host Microbe* **22**, 653–666.e5 (2017). doi: [10.1016/j.chom.2017.10.006](https://doi.org/10.1016/j.chom.2017.10.006); pmid: [29120743](https://pubmed.ncbi.nlm.nih.gov/29120743/)
60. Y. Xing *et al.*, Molecular Signature of Pruriceptive MrgprA3<sup>+</sup> Neurons. *J. Invest. Dermatol.* **140**, 2041–2050 (2020). doi: [10.1016/j.jid.2020.03.935](https://doi.org/10.1016/j.jid.2020.03.935); pmid: [32234460](https://pubmed.ncbi.nlm.nih.gov/32234460/)
61. L. J. Elias *et al.*, Touch neurons underlying dopaminergic pleasurable touch and sexual receptivity. *Cell* **186**, 577–590.e16 (2023). doi: [10.1016/j.cell.2022.12.034](https://doi.org/10.1016/j.cell.2022.12.034); pmid: [36693373](https://pubmed.ncbi.nlm.nih.gov/36693373/)
62. E. F. Webb, M. N. Tzimas, D. E. Griswold, S. J. Newsholme, Intralesional cytokines in chronic oxazolone-induced contact sensitivity suggest roles for tumor necrosis factor  $\alpha$  and interleukin-4. *J. Invest. Dermatol.* **111**, 86–92 (1998). doi: [10.1046/j.1523-1747.1998.00239.x](https://doi.org/10.1046/j.1523-1747.1998.00239.x); pmid: [9665392](https://pubmed.ncbi.nlm.nih.gov/9665392/)
63. K. De Filippo *et al.*, Mast cell and macrophage chemokines CXCL1/CXCL2 control the early stage of neutrophil recruitment during tissue inflammation. *Blood* **121**, 4930–4937 (2013). doi: [10.1182/blood-2013-02-486217](https://doi.org/10.1182/blood-2013-02-486217); pmid: [23645836](https://pubmed.ncbi.nlm.nih.gov/23645836/)
64. M. Bandyopadhyay *et al.*, Skin codelivery of contact sensitizers and neurokinin-1 receptor antagonists integrated in microneedle arrays suppresses allergic contact dermatitis. *J. Allergy Clin. Immunol.* **150**, 114–130 (2022). doi: [10.1016/j.jaci.2021.12.794](https://doi.org/10.1016/j.jaci.2021.12.794); pmid: [35085664](https://pubmed.ncbi.nlm.nih.gov/35085664/)
65. T. Numata, K. Harada, S. Nakae, Roles of Mast Cells in Cutaneous Diseases. *Front. Immunol.* **13**, 923495 (2022). doi: [10.3389/fimmu.2022.923495](https://doi.org/10.3389/fimmu.2022.923495); pmid: [35874756](https://pubmed.ncbi.nlm.nih.gov/35874756/)
66. J. Scholten *et al.*, Mast cell-specific Cre/loxP-mediated recombination in vivo. *Transgenic Res.* **17**, 307–315 (2008). doi: [10.1007/s11248-007-9153-4](https://doi.org/10.1007/s11248-007-9153-4); pmid: [17972156](https://pubmed.ncbi.nlm.nih.gov/17972156/)
67. T. D. Sheahan, C. A. Warwick, L. G. Fanien, S. E. Ross, The Neurokinin-1 Receptor is Expressed with Gastrin-Releasing Peptide Receptor in Spinal Interneurons and Modulates Itch. *J. Neurosci.* **40**, 8816–8830 (2020). doi: [10.1523/JNEUROSCI.1832-20.2020](https://doi.org/10.1523/JNEUROSCI.1832-20.2020); pmid: [33051347](https://pubmed.ncbi.nlm.nih.gov/33051347/)
68. S. Zhang *et al.*, Nonpeptidergic neurons suppress mast cells via glutamate to maintain skin homeostasis. *Cell* **184**, 2151–2166.e16 (2021). doi: [10.1016/j.cell.2021.03.002](https://doi.org/10.1016/j.cell.2021.03.002); pmid: [33765440](https://pubmed.ncbi.nlm.nih.gov/33765440/)
69. E. Azimi *et al.*, Dual action of neurokinin-1 antagonists on Mas-related GPCRs. *JCI Insight* **1**, e89362 (2016). doi: [10.1172/jci.insight.89362](https://doi.org/10.1172/jci.insight.89362); pmid: [27734033](https://pubmed.ncbi.nlm.nih.gov/27734033/)
70. O. Malbec *et al.*, Peritoneal cell-derived mast cells: An in vitro model of mature serosal-type mouse mast cells. *J. Immunol.* **178**, 6465–6475 (2007). doi: [10.4049/jimmunol.178.10.6465](https://doi.org/10.4049/jimmunol.178.10.6465); pmid: [17475876](https://pubmed.ncbi.nlm.nih.gov/17475876/)
71. H. M. Fugate, J. M. Kapfer, R. W. McLaughlin, Analysis of the Microbiota in the Fecal Material of Painted Turtles (*Chrysemys picta*). *Curr. Microbiol.* **77**, 11–14 (2020). doi: [10.1007/s00284-019-01787-5](https://doi.org/10.1007/s00284-019-01787-5); pmid: [31642965](https://pubmed.ncbi.nlm.nih.gov/31642965/)
72. M. Meisel *et al.*, Microbial signals drive pre-leukaemic myeloproliferation in a Tet2-deficient host. *Nature* **557**, 580–584 (2018). doi: [10.1038/s41586-018-0125-z](https://doi.org/10.1038/s41586-018-0125-z); pmid: [29769727](https://pubmed.ncbi.nlm.nih.gov/29769727/)

## ACKNOWLEDGMENTS

We thank K. Albers, B. Davis, and T. Hand as well as other members of the University of Pittsburgh Center for Pain Research and the Departments of Dermatology and Immunology for helpful discussions. We also thank the Division of Laboratory Animal Resources of the University of Pittsburgh for excellent animal care. BioRender.com was used to create figs. S5 and S9. **Funding:** This work was supported by National Institutes of Health (NIH) grants T32NS73548 (A.W.L.), T32CA082084 (C.M.P.), R01DK130897 (M.M.), U24EV035102 (M.M.), R01AR063772 (S.E.R.), K99NS126569 (T.D.S.), R01AR071720 (D.H.K.), and R01AR077341 (D.H.K.). This work was supported by the Deutsche Forschungsgemeinschaft (DFG, German Research Foundation) (T.R.). **Author contributions:** A.W.L., M.M., and D.H.K. designed and interpreted experiments. A.W.L., Y.R.Z., C.-S.C., T.N.E., S.O., T.R., L.M.M., E.S.W., J.E.G., C.R.L., J.K., S.K.R., C.M.P., K.K., S.-L.N.N., and H.M.K. performed experiments. S.E.R., T.D.S., and T.L.S. provided technical and conceptual assistance. A.W.L. and D.H.K. wrote the manuscript, and all authors edited it. **Competing interests:** Patents with D.H.K. as inventor have been filed by the University of Pittsburgh describing the use of Glnk2 agonism to suppress mast cell function and the use and formulation of  $\beta$ -alanine to suppress mast cell function. D.H.K. is a paid consultant for AbbVie, Inc; Beiersdorf AG; Janssen Research and Development, LLC; and Adition Bio. D.H.K. has a sponsored research agreement with Galderma Laboratories, Lp. T.L.S. is a paid consultant for Panther Life Sciences, LTD. The authors declare no other competing interests. **Data and materials availability:** All data needed to evaluate the conclusions in the paper are present in the paper or the supplementary materials. 16S rRNA-seq data are available at the National Center for Biotechnology Information (NCBI) Sequence Read Archive (PRJNA1179991). **License information:** Copyright © 2025 the authors, some rights reserved; exclusive licensee American Association for the Advancement of Science. No claim to original US government works. <https://www.science.org/about/science-licenses-journal-article-reuse>

## SUPPLEMENTARY MATERIALS

[science.org/doi/10.1126/science.adn9390](https://science.org/doi/10.1126/science.adn9390)

Figs. S1 to S9

MDAR Reproducibility Checklist

Submitted 8 January 2024; resubmitted 22 September 2024

Accepted 3 December 2024

[10.1126/science.adn9390](https://doi.org/10.1126/science.adn9390)